

## Convexification Numerical Method for a Coefficient Inverse Problem for the Radiative Transport Equation\*

Michael V. Klibanov<sup>†</sup>, Jingzhi Li<sup>‡</sup>, Loc H. Nguyen<sup>†</sup>, and Zhipeng Yang<sup>§</sup>

**Abstract.** An  $(n+1)$ -D coefficient inverse problem for the stationary radiative transport equation is considered for the first time. A globally convergent so-called convexification numerical method is developed and its convergence analysis is provided. The analysis is based on a Carleman estimate. Extensive numerical studies in the two-dimensional case are presented.

**Key words.** coefficient inverse problem, radiative transport equation, convexification method, special orthonormal basis, global convergence analysis, numerical experiments

**MSC codes.** 35R30, 65M32

**DOI.** 10.1137/22M1509837

**1. Introduction.** The stationary radiative transfer equation (RTE) governs the propagation of the radiation field in media with absorbing, emitting, and scattering radiation. RTE has broad applications in optics, including diffuse optical tomography [16], astrophysics, atmospheric science, and other applied disciplines. For example, in single particle emission tomography the coefficient we reconstruct is the emission coefficient [29, formula (2.1)]. The RTE we consider here is a more general one since we introduce an integral operator in it.

For the first time, we develop in this paper a globally convergent numerical method for a coefficient inverse problem (CIP) of the recovery of a spatially distributed coefficient of RTE in the  $(n+1)$ -D case,  $n \geq 1$ . All CIPs are both nonlinear and ill-posed. Numerical methods for inverse source problems for RTE were developed in [10, 11, 12, 31]. In the case of single particle emission tomography, i.e., when the kernel of the integral operator in RTE is the identical zero function, an inversion formula for the inverse source problem was derived in [30] and tested numerically in [15]. Inverse problems of [10, 11, 12, 15, 30, 31] are linear ones.

\* Received by the editors July 18, 2022; accepted for publication (in revised form) September 26, 2022; published electronically January 19, 2023.

<https://doi.org/10.1137/22M1509837>

**Funding:** The work of the second author was partially supported by National Natural Science Foundation of China grant 11971221, Guangdong NSF Major Fund 2021ZDZX1001, and Shenzhen Sci-Tech Funds R-CJC20200714114556020, JCYJ20200109115422828, and JCYJ20190809150413261. The work of the third author was partially supported by National Science Foundation grant DMS-2208159 and the Faculty Research Grant program at UNC Charlotte, fund 111272.

<sup>†</sup> Department of Mathematics and Statistics, University of North Carolina at Charlotte, Charlotte, NC 28223 USA ([mklibanv@uncc.edu](mailto:mklibanv@uncc.edu), [loc.nguyen@uncc.edu](mailto:loc.nguyen@uncc.edu)).

<sup>‡</sup> Corresponding author. Department of Mathematics, National Center for Applied Mathematics Shenzhen, SUSTech International Center for Mathematics, Southern University of Science and Technology, Shenzhen 518055, People's Republic of China ([li.jz@sustech.edu.cn](mailto:li.jz@sustech.edu.cn)).

<sup>§</sup> Department of Mathematics, Southern University of Science and Technology, Shenzhen 518055, People's Republic of China ([yangzp@sustech.edu.cn](mailto:yangzp@sustech.edu.cn)).

Our CIP is formally determined, i.e., the number of free variables in the data equals the number of free variables in the unknown coefficient. Our data are incomplete, i.e., the source runs along an interval of a straight line and the data are measured only at a part of the boundary  $\partial\Omega$  of the domain of interest  $\Omega$ .

We now comment on some uniqueness and stability results for inverse problems for RTE. Both our discussion and the number of references to corresponding results are limited since this topic is outside of the scope of the current paper. In the case when the source function is unknown in the stationary RTE, we refer to [3, 32], where some uniqueness theorems are proven. In the case when a coefficient of the stationary RTE is unknown, we refer to [2] for some stability results. In the case of CIPs for the time dependent RTE, some uniqueness and stability theorems were proven in [13, 27, 28] using some modifications of the technique of [7].

The goal of this paper is to construct a globally convergent numerical method for our CIP, to conduct its convergence analysis, and to confirm our method via numerical experiments. To achieve this goal, we develop in this paper a new version of the so-called convexification method [25]. The convexification constructs a least squares cost functional, which is strictly convex on a bounded convex set in an appropriate Hilbert space. The diameter of this set is fixed and is an arbitrary number. We prove existence and uniqueness of the minimizer of that functional on that set and estimate convergence rate of minimizers to the true solution depending on the level of the noise in the data. As a by-product, we obtain a certain uniqueness result for our CIP. Also, we establish the global convergence of the gradient descent method of the minimization of our functional. Recall that only local convergence of this method can be proven in the nonconvex case. In addition, we present numerical experiments in the two-dimensional case.

We call a numerical method for a CIP *globally convergent* if a theorem is proven, which claims that this method delivers at least one point in a sufficiently small neighborhood of the solution of this CIP without an advanced knowledge of that neighborhood; also, see [25, Definition 1.4.2] for a similar statement.

Conventional numerical methods for CIPs are based on the minimization of least squares cost functionals; see, e.g., [8, 14]. However, these functionals are usually nonconvex, thus they typically have multiple local minima and ravines. It is well known that this complicates the problem of their optimization. These considerations prompted the first author to work on the developments of the convexification technique in previous publications [21, 23].

The convexification uses the idea of the so-called Bukhgeim-Klibanov method (BK), which is based on Carleman estimates; see, e.g., the books [4, 25] for Carleman estimates. BK was originally introduced in the field of CIPs in 1981 [7] only for the proofs of uniqueness theorems for multidimensional CIPs. The work [7] has generated many publications by many authors since then; see, e.g., the books [4, 25] and references cited therein. The majority of currently known publications about BK are also dedicated to the issues of uniqueness and stability of CIPs. Unlike these, it was proposed in [21, 23] to use the idea of BK for the construction of the above mentioned globally strictly convex cost functionals for CIPs. Starting from the work [1], which has removed some obstacles for real computations, a number of works have been published, which combine the theory and computations of convexification; see, e.g., [6, 20, 24, 25, 26] and references cited therein.

Let  $B$  be a Banach space and  $s \geq 2$  be an integer. Below the space  $B_s$  is defined as

$$B_s = \left\{ f = (f_1, \dots, f_s)^T, f_i \in B, i = 1, \dots, s \right\}, \|f\|_{B_s} = \left( \sum_{i=1}^s \|f_i\|_B^2 \right)^{1/2}.$$

All functions considered below are real valued ones. In section 2 we pose forward and inverse problems and prove existence and uniqueness theorems for the solution of the forward problem. In section 3 we describe our transformation procedure. In section 4 we introduce our convexification functional and formulate five theorems. These theorems are proven in section 5. In section 6 we present our numerical results.

**2. Statements of forward and inverse problems.** For  $n \geq 1$ , points in  $\mathbb{R}^{n+1}$  are denoted below as  $\mathbf{x} = (x_1, x_2, \dots, x_n, y) \in \mathbb{R}^{n+1}$ . Let numbers  $A, a, b, d > 0$ , where

$$(2.1) \quad 1 < a < b.$$

Define the rectangular prism  $\Omega \subset \mathbb{R}^{n+1}$  and parts  $\partial_1\Omega, \partial_2\Omega, \partial_3\Omega$  of its boundary  $\partial\Omega$  as

$$(2.2) \quad \Omega = \{ \mathbf{x} : -A < x_1, \dots, x_n < A, a < y < b \},$$

$$(2.3) \quad \partial_1\Omega = \{ \mathbf{x} : -A < x_1, \dots, x_n < A, y = a \},$$

$$(2.4) \quad \partial_2\Omega = \{ \mathbf{x} : -A < x_1, \dots, x_n < A, y = b \},$$

$$(2.5) \quad \partial_3\Omega = \{ x_i = \pm A, y \in (a, b), i = 1, \dots, n, \}.$$

Let  $\Gamma_d$  be the line where the external sources are

$$(2.6) \quad \Gamma_d = \{ \mathbf{x}_\alpha = (\alpha, 0, \dots, 0) : \alpha \in [-d, d] \}.$$

Hence,  $\Gamma_d$  is a part of the  $x_1$ -axis. It follows from (2.1) and (2.2) that  $\Gamma_d \cap \bar{\Omega} = \emptyset$ .

Let the points of external sources  $\mathbf{x}_\alpha$  run along  $\Gamma_d$ ,  $\mathbf{x}_\alpha \in \Gamma_d$ . Let  $\varepsilon > 0$  be a sufficiently small number. To avoid dealing with singularities, we model the  $\delta(\mathbf{x})$ -function as

$$(2.7) \quad f(\mathbf{x}) = C_\varepsilon \begin{cases} \exp\left(\frac{|\mathbf{x}|^2}{\varepsilon^2 - |\mathbf{x}|^2}\right), & |\mathbf{x}| < \varepsilon, \\ 0, & |\mathbf{x}| \geq \varepsilon, \end{cases}$$

where the constant  $C_\varepsilon$  is chosen such that

$$(2.8) \quad C_\varepsilon \int_{|\mathbf{x}| < \varepsilon} \exp\left(\frac{|\mathbf{x}|^2}{\varepsilon^2 - |\mathbf{x}|^2}\right) d\mathbf{x} = 1.$$

Hence, the function  $f(\mathbf{x} - \mathbf{x}_\alpha) = f(x_1 - \alpha, x_2, \dots, x_n, y) \in C^\infty(\mathbb{R}^{n+1})$  plays the role of the source function for the source  $\mathbf{x}_\alpha$ . We choose  $\varepsilon$  so small that

$$(2.9) \quad f(\mathbf{x} - \mathbf{x}_\alpha) = 0 \quad \forall \mathbf{x} \in \bar{\Omega} \forall \mathbf{x}_\alpha \in \Gamma_d.$$

Let  $A_1 = \max(A, d)$ . Introduce three domains  $G \subset \mathbb{R}^{n+1}$  and  $G_a^+, G_a^- \subset G$ ,

$$(2.10) \quad G = \{\mathbf{x} : |x_1|, \dots, |x_n| < A_1, y \in (0, b)\}, G_a^+ = G \cap \{y > a\}, G_a^- = G \setminus G_a^+.$$

By (2.2), (2.6), and (2.10)  $\Omega \subset G_a^+$ . By (2.15), (2.16), and (2.10)  $a(\mathbf{x}) = 0$  for  $\mathbf{x} \in G \setminus \Omega$ . Everywhere below

$$(2.11) \quad (\mathbf{x}, \alpha) \in G \times (-d, d).$$

Let  $u(\mathbf{x}, \alpha)$  denote the steady-state radiance at the point  $\mathbf{x}$  generated by the source function  $f(\mathbf{x} - \mathbf{x}_\alpha)$ . We assume that the function  $u(\mathbf{x}, \alpha)$  is governed by the stationary RTE of the following form [16]:

$$(2.12) \quad \begin{aligned} & \nu(\mathbf{x}, \alpha) \cdot \nabla_{\mathbf{x}} u(\mathbf{x}, \alpha) + a(\mathbf{x})u(\mathbf{x}, \alpha) \\ &= \mu_s(\mathbf{x}) \int_{\Gamma_d} K(\mathbf{x}, \alpha, \beta)u(\mathbf{x}, \beta)d\beta + f(\mathbf{x} - \mathbf{x}_\alpha), \mathbf{x} \in G, \mathbf{x}_\alpha \in \Gamma_d. \end{aligned}$$

The kernel  $K(\mathbf{x}, \alpha, \beta)$  of the integral operator in (2.12) is called the “phase function,”

$$(2.13) \quad K(\mathbf{x}, \alpha, \beta) \geq 0, \mathbf{x} \in \overline{G}; \alpha, \beta \in [-d, d];$$

see [16]. In addition, we assume that

$$(2.14) \quad K(\mathbf{x}, \alpha, \beta) \in C^1(\overline{G} \times [-d, d]^2).$$

In (2.12),

$$(2.15) \quad a(\mathbf{x}) = \mu_a(\mathbf{x}) + \mu_s(\mathbf{x}),$$

where  $\mu_a(\mathbf{x})$  and  $\mu_s(\mathbf{x})$  are the absorption and scattering coefficients, respectively, and  $a(\mathbf{x})$  is the emission coefficient [29, formula (2.1)]. We assume that

$$(2.16) \quad \mu_a(\mathbf{x}), \mu_s(\mathbf{x}) \geq 0, \mu_a(\mathbf{x}) = \mu_s(\mathbf{x}) = 0, \mathbf{x} \in G \setminus \Omega,$$

$$(2.17) \quad \mu_a(\mathbf{x}), \mu_s(\mathbf{x}) \in C^1(\overline{G}).$$

For two arbitrary points  $\mathbf{x}, \mathbf{z} \in \mathbb{R}^{n+1}$  let  $L(\mathbf{x}, \mathbf{z})$  be the line segment connecting these points and let  $ds$  be the element of the euclidean length on  $L(\mathbf{x}, \mathbf{z})$ . In (2.12)  $\nu(\mathbf{x}, \alpha)$  denotes the unit vector, which is parallel to  $L(\mathbf{x}, \mathbf{x}_\alpha)$ ,

$$(2.18) \quad \nu(\mathbf{x}, \alpha) = \frac{\mathbf{x} - \mathbf{x}_\alpha}{|\mathbf{x} - \mathbf{x}_\alpha|}.$$

**Forward problem.** Let (2.1)–(2.18) hold. Find the function  $u(\mathbf{x}, \alpha) \in C^1(\overline{G} \times [-d, d])$  satisfying (2.12) and the initial condition

$$(2.19) \quad u(\mathbf{x}_\alpha, \alpha) = 0 \text{ for } \mathbf{x}_\alpha \in \Gamma_d.$$

**Coefficient inverse problem.** Let (2.1)–(2.18) hold. Let the function  $u(\mathbf{x}, \alpha) \in C^1(\overline{G} \times [-d, d])$  be the solution of the forward problem. Assume that the coefficient  $a(\mathbf{x})$  of (2.12) is unknown. Determine the function  $a(\mathbf{x})$ , assuming that the following function  $g(\mathbf{x}, \alpha)$  is known:

$$(2.20) \quad g(\mathbf{x}, \alpha) = u(\mathbf{x}, \alpha) \quad \forall \mathbf{x} \in \partial\Omega \setminus \partial_1\Omega \quad \forall \alpha \in (-d, d).$$

*Remark 2.1.* This CIP is an ill-posed one, like all other CIPs. However, we are unaware of any expectations of the nature of the ill-posedness of our specific CIP. This question is outside of the scope of the current paper and needs to be investigated separately.

First, we formulate and prove an existence and uniqueness theorem for the solution of the forward problem. Some other existence results for the stationary RTE were proven in [31, 32]. Unlike Theorem 2.1, the positivity of the function  $u$  was not discussed in [31, 32]. On the other hand, we need this property of  $u$  for our numerical method.

**Theorem 2.1.** Assume that (2.1), (2.2), (2.6)–(2.9), and (2.13)–(2.17) hold. Then there exists unique solution  $u(\mathbf{x}, \alpha) \in C^1(\overline{G} \times [-d, d])$  of (2.12) with the initial condition (2.19). Furthermore, the following inequality holds:

$$(2.21) \quad u(\mathbf{x}, \alpha) \geq m > 0 \text{ for } (\mathbf{x}, \alpha) \in \overline{G}_a^+ \times [-d, d],$$

$$(2.22) \quad m = \min_{\overline{G}_a^+ \times [-d, d]} \left[ \exp \left( - \int_{L(\mathbf{x}, \mathbf{x}_\alpha)} a(\mathbf{x}(s)) ds \right) \cdot \left( \int_{L(\mathbf{x}, \mathbf{x}_\alpha)} f(\mathbf{x}(s) - \mathbf{x}_\alpha) ds \right) \right].$$

*Proof.* Recall (2.11). Equation (2.12) can be rewritten as

$$(2.23) \quad D_\nu u(\mathbf{x}, \alpha) + a(\mathbf{x})u(\mathbf{x}, \alpha) = \mu_s(\mathbf{x}) \int_{\Gamma_d} K(\mathbf{x}, \alpha, \beta)u(\mathbf{x}, \beta)d\beta + f(\mathbf{x} - \mathbf{x}_\alpha),$$

where  $D_\nu$  is the operator of the directional derivative in the direction of the vector  $\nu(\mathbf{x}, \alpha)$ . We can consider (2.23) as the first order linear ordinary differential operator along the line segment  $L(\mathbf{x}, \mathbf{x}_\alpha)$ . Denote

$$(2.24) \quad p(\mathbf{x}, \alpha) = \int_{L(\mathbf{x}, \mathbf{x}_\alpha)} a(\mathbf{x}(s))ds, \quad c(\mathbf{x}, \alpha) = e^{p(\mathbf{x}, \alpha)}.$$

Obviously,  $L(\mathbf{x}, \mathbf{x}_\alpha) = \{\mathbf{z}(t) = (\alpha + t(x_1 - \alpha), tx_2, \dots, tx_n, ty), t \in (0, 1)\}$ . Hence,  $ds = |\mathbf{x} - \mathbf{x}_\alpha|dt$  in (2.24). We obtain

$$(2.25) \quad p(\mathbf{x}, \alpha) = |\mathbf{x} - \mathbf{x}_\alpha| \int_0^1 a(\alpha + t(x_1 - \alpha), tx_2, \dots, tx_n, ty) dt.$$

Since by (2.15) and (2.17)  $a \in C^1(\overline{G})$ , then (2.18), (2.24), (2.25), and elementary calculations imply that  $D_\nu p(\mathbf{x}, \alpha) = a(\mathbf{x})$ . Consider now the integration factor  $c(\mathbf{x}, \alpha)$  defined in (2.24). By (2.24)  $D_\nu c(\mathbf{x}, \alpha) = a(\mathbf{x})c(\mathbf{x}, \alpha)$ . Multiplying both sides of (2.23) by  $c(\mathbf{x}, \alpha)$ , we obtain

$$(2.26) \quad \begin{aligned} & c(\mathbf{x}, \alpha)D_\nu u(\mathbf{x}, \alpha) + c(\mathbf{x}, \alpha)a(\mathbf{x})u(\mathbf{x}, \alpha) \\ & = c(\mathbf{x}, \alpha)\mu_s(\mathbf{x}) \int_{\Gamma_d} K(\mathbf{x}, \alpha, \beta)u(\mathbf{x}, \beta)d\beta + c(\mathbf{x}, \alpha)f(\mathbf{x} - \mathbf{x}_\alpha). \end{aligned}$$

We have

$$(2.27) \quad cD_\nu u + cau = D_\nu(cu) - uD_\nu c + cau = D_\nu(cu) - cau + cau = D_\nu(cu).$$

Since by (2.7)–(2.9), (2.15), (2.16), and (2.24)  $c(\mathbf{x}, \alpha) = 1$  for all points  $\mathbf{x}$  where  $f(\mathbf{x} - \mathbf{x}_\alpha) \neq 0$ , then  $c(\mathbf{x}, \alpha)f(\mathbf{x} - \mathbf{x}_\alpha) = f(\mathbf{x} - \mathbf{x}_\alpha)$ . Hence, (2.2), (2.10), (2.11), (2.15), (2.16), and (2.27) imply that (2.26) is equivalent with

$$(2.28) \quad D_\nu((cu)(\mathbf{x}, \alpha)) = c(\mathbf{x}, \alpha)\mu_s(\mathbf{x}) \int_{\Gamma_d} K(\mathbf{x}, \alpha, \beta)u(\mathbf{x}, \beta)d\beta + f(\mathbf{x} - \mathbf{x}_\alpha).$$

Integrating (2.28) over the line  $L(\mathbf{x}, \mathbf{x}_\alpha)$  and using the initial condition (2.19), we obtain

$$(2.29) \quad \begin{aligned} u(\mathbf{x}, \alpha) &= u_0(\mathbf{x}, \alpha) \\ &+ \frac{1}{c(\mathbf{x}, \alpha)} \int_{L(\mathbf{x}, \mathbf{x}_\alpha)} c(\mathbf{x}(s), \alpha)\mu_s(\mathbf{x}(s)) \left( \int_{\Gamma_d} K(\mathbf{x}(s), \alpha, \beta)u(\mathbf{x}(s), \beta)d\beta \right) ds, \end{aligned}$$

$$(2.30) \quad u_0(\mathbf{x}, \alpha) = \frac{1}{c(\mathbf{x}, \alpha)} \int_{L(\mathbf{x}, \mathbf{x}_\alpha)} f(\mathbf{x}(s) - \mathbf{x}_\alpha) ds = e^{-p(\mathbf{x}, \alpha)} \int_{L(\mathbf{x}, \mathbf{x}_\alpha)} f(\mathbf{x}(s) - \mathbf{x}_\alpha) ds.$$

It follows from (2.15), (2.16), (2.24), (2.29), and (2.30) that

$$(2.31) \quad u(\mathbf{x}, \alpha) = u_0(\mathbf{x}, \alpha) = \int_{L(\mathbf{x}, \mathbf{x}_\alpha)} f(\mathbf{x}(s) - \mathbf{x}_\alpha) ds, \quad (\mathbf{x}, \alpha) \in G_a^- \times (-d, d).$$

By (2.7) and (2.8)  $f \geq 0$ . Hence, (2.24) and (2.30) imply

$$(2.32) \quad u_0(\mathbf{x}, \alpha) \geq m, \quad (\mathbf{x}, \alpha) \in \overline{G}_a^+ \times [-d, d],$$

where the number  $m$  is defined in (2.22). It follows from the above construction that the problem (2.29), (2.30) is equivalent with the problem (2.12), (2.19).

Similarly with (2.24) and (2.25), for  $\mathbf{x} \in G_a^+$  and for any appropriate function  $\varphi(\mathbf{z})$

$$\begin{aligned} \int_{L(\mathbf{x}, \mathbf{x}_\alpha)} \varphi(\mathbf{z}(s)) ds &= |\mathbf{x} - \mathbf{x}_\alpha| \int_0^1 \varphi\left(\alpha + t(x_1 - \alpha), tx_2, \dots, tx_n, ty\right) dt \\ &= \frac{|\mathbf{x} - \mathbf{x}_\alpha|}{y} \int_0^y \varphi\left(\alpha + \frac{(x_1 - \alpha)}{y}z, \frac{x_2}{y}z, \dots, \frac{x_n}{y}z, z\right) dz \\ &= \frac{|\mathbf{x} - \mathbf{x}_\alpha|}{y} \int_0^a \varphi\left(\alpha + \frac{(x_1 - \alpha)}{y}z, \frac{x_2}{y}z, \dots, \frac{x_n}{y}z, z\right) dz \\ &\quad + \frac{|\mathbf{x} - \mathbf{x}_\alpha|}{y} \int_a^y \varphi\left(\alpha + \frac{(x_1 - \alpha)}{y}z, \frac{x_2}{y}z, \dots, \frac{x_n}{y}z, z\right) dz. \end{aligned}$$

Hence, (2.29) and (2.30) imply

$$(2.33) \quad \begin{aligned} u(x_1, x_2, \dots, y, \alpha) &= u_0(\mathbf{x}, \alpha) \\ &+ \frac{|\mathbf{x} - \mathbf{x}_\alpha|}{yc(\mathbf{x})} \int_a^y (c\mu_s)(\mathbf{x}(z), \alpha) \left( \int_{\Gamma_d} K(\mathbf{x}(z), \alpha, \beta)u(\mathbf{x}(z), \beta)d\beta \right) dz, \end{aligned}$$

$$(2.34) \quad \mathbf{x}(z) = \left( \alpha + \frac{(x_1 - \alpha)}{y} z, \frac{x_2}{y} z, \dots, \frac{x_n}{y} z, z \right),$$

where  $(\mathbf{x}, \alpha) \in G_a^+ \times (-d, d)$ . Thus, we have obtained the  $\alpha$ -dependent family of integral equations (2.33), (2.34) of the Volterra type in the bounded domain  $G_a^+$ . Furthermore, any solution of problem (2.30), (2.31), (2.33), (2.34) satisfies (2.12) with the initial condition (2.19). Therefore, to solve the forward problem, it is sufficient to solve problem (2.33), (2.34). It follows from the well-known classical results about Volterra equations that there exists unique function  $u(\mathbf{x}, \alpha) \in C(\overline{G}_a^+ \times [-d, d])$  satisfying (2.33), (2.34), and this function can be obtained via the following iterative process:

$$(2.35) \quad \begin{aligned} u_n(\mathbf{x}, \alpha) &= u_0(\mathbf{x}, \alpha) \\ &+ \frac{|\mathbf{x} - \mathbf{x}_\alpha|}{y c(\mathbf{x}, \alpha)} \int_a^y (c \mu_s)(\mathbf{x}(z), \alpha) \left( \int_{\Gamma_d} K(\mathbf{x}(z), \alpha, \beta) u_{n-1}(\mathbf{x}(z), \beta) d\beta \right) dz, \end{aligned}$$

where  $(\mathbf{x}, \alpha) \in G_a^+ \times (-d, d)$  and  $n = 1, 2, \dots$ . It follows from (2.35) that

$$(2.36) \quad |u_n(\mathbf{x}, \alpha)| \leq \sum_{k=0}^n \frac{(M_1(y-a))^k}{k!}, \quad (\mathbf{x}, \alpha) \in \overline{G}_a^+ \times [-d, d], n = 0, 1, \dots,$$

where the number  $M_1 = M_1(A, a, b, d, \|a(\mathbf{x})\|_{C(\overline{\Omega})}, \|K\|_{C(\overline{\Omega} \times [-d, d]^2)}, \|f\|_{C(|\mathbf{x}| \leq \varepsilon)}) > 0$  depends only on listed parameters. Next, (2.13), (2.15), (2.16), (2.22), (2.24), (2.30), (2.32), and (2.35) imply that  $u_n(\mathbf{x}, \alpha) \geq m, n = 0, 1, \dots$  for  $(\mathbf{x}, \alpha) \in \overline{G}_a^+ \times [-d, d]$ . Therefore, (2.36) implies that estimate (2.21) holds. Next, it follows from (2.14), (2.17), and (2.35) that functions  $u_n(\mathbf{x}, \alpha)$  can be differentiated once with respect to  $x_1, \dots, x_n, y, \alpha$  and, similarly with (2.36), the following estimates hold for  $\mathbf{n} = \mathbf{0}, \mathbf{1} \dots$ :

$$(2.37) \quad |\nabla_{\mathbf{x}} u_n(\mathbf{x}, \alpha)|, |\partial_\alpha u_n(\mathbf{x}, \alpha)| \leq \sum_{k=0}^n \frac{(M_2(y-a))^k}{k!}, \quad (\mathbf{x}, \alpha) \in \overline{G}_a^+ \times [-d, d],$$

Here, the number  $M_2 = M_2(A, a, b, d, \|a(\mathbf{x})\|_{C^1(\overline{\Omega})}, \|K\|_{C^1(\overline{\Omega} \times [-d, d]^2)}, \|f\|_{C^1(|\mathbf{x}| \leq \varepsilon)}) > 0$  depends only on listed parameters. Estimates (2.36) and (2.37) combined with (2.31) imply that we have found the unique function  $u(\mathbf{x}, \alpha) \in C^1(\overline{G} \times [-d, d])$  satisfying (2.12) and the initial condition (2.19). Furthermore, estimate (2.21) with the number  $m$  defined in (2.22) is proven.  $\blacksquare$

### 3. Transformation.

**3.1. An integral differential equation without the unknown coefficient  $a(\mathbf{x})$ .** The first step of the convexification is a transformation of the above CIP to a boundary value problem for a certain PDE of the second order, in which the unknown coefficient  $a(\mathbf{x})$  is not involved. By (2.21) we can introduce a new function  $w(\mathbf{x}, \alpha)$ ,

$$(3.1) \quad w(\mathbf{x}, \alpha) = \ln u(\mathbf{x}, \alpha), \quad (\mathbf{x}, \alpha) \in \overline{\Omega} \times [-d, d].$$

Substituting (3.1) in (2.12) and (2.20), we obtain

$$(3.2) \quad \begin{aligned} \nu(\mathbf{x}, \alpha) \cdot \nabla_{\mathbf{x}} w(\mathbf{x}, \alpha) + a(\mathbf{x}) \\ = e^{-w(\mathbf{x}, \alpha)} \mu_s(\mathbf{x}) \int_{\Gamma_d} K(\mathbf{x}, \alpha, \beta) e^{w(\mathbf{x}, \beta)} d\beta, \quad \mathbf{x} \in \Omega, \alpha \in (-d, d), \end{aligned}$$

$$(3.3) \quad w(\mathbf{x}, \alpha) |_{\partial\Omega} = \ln g_1(\mathbf{x}, \alpha),$$

$$(3.4) \quad g_1(\mathbf{x}, \alpha) = \begin{cases} g(\mathbf{x}, \alpha), \mathbf{x} \in \partial\Omega \setminus \partial_1\Omega, \alpha \in (-d, d), \\ u_0(\mathbf{x}, \alpha), \mathbf{x} \in \partial_1\Omega, \alpha \in (-d, d). \end{cases}$$

Differentiate both sides of (3.3) with respect to  $\alpha$  and use  $\partial_\alpha a(\mathbf{x}) \equiv 0$ . We obtain an integral differential equation with the derivatives up to the second order,

$$(3.5) \quad \begin{aligned} & \nu(\mathbf{x}, \alpha) \cdot \nabla_{\mathbf{x}} w_{\alpha}(\mathbf{x}, \alpha) + \partial_{\alpha} \nu(\mathbf{x}, \alpha) \cdot \nabla_{\mathbf{x}} w(\mathbf{x}, \alpha) \\ &= \mu_s(\mathbf{x}) \frac{\partial}{\partial \alpha} \left[ e^{-w(\mathbf{x}, \alpha)} \int_{\Gamma_d} K(\mathbf{x}, \alpha, \beta) e^{w(\mathbf{x}, \beta)} d\beta \right], \mathbf{x} \in \Omega, \alpha \in (-d, d). \end{aligned}$$

We have  $\nu(\mathbf{x}, \alpha) = (\nu_1(\mathbf{x}, \alpha), \nu_2(\mathbf{x}, \alpha), \dots, \nu_{n+1}(\mathbf{x}, \alpha))$ , where by (2.18)

$$\begin{aligned} \nu_1(\mathbf{x}, \alpha) &= (x_1 - \alpha) \left[ (x_1 - \alpha)^2 + x_2^2 + \dots + x_n^2 + y^2 \right]^{-1/2}, \\ \nu_k(\mathbf{x}, \alpha) &= x_k \left[ (x_1 - \alpha)^2 + x_2^2 + \dots + x_n^2 + y^2 \right]^{-1/2}, \quad k = 2, \dots, n, \\ \nu_{n+1}(\mathbf{x}, \alpha) &= y \left[ (x_1 - \alpha)^2 + x_2^2 + \dots + x_n^2 + y^2 \right]^{-1/2}. \end{aligned}$$

Hence, (2.1)–(2.6) imply that with a constant  $M_3 = M_3(A, d) > 0$  depending only on numbers  $A, d$  the following estimates are valid:

$$(3.6) \quad \left| \frac{\partial_{\alpha} \nu_k(\mathbf{x}, \alpha)}{\nu_{n+1}(\mathbf{x}, \alpha)} \right|, \left| \frac{\nu_k(\mathbf{x}, \alpha)}{\nu_{n+1}(\mathbf{x}, \alpha)} \right| \leq \frac{M_3}{a}, \quad k = 1, \dots, n, \mathbf{x} \in \bar{\Omega}, \alpha \in [-d, d].$$

**3.2. An orthonormal basis in  $L^2(-d, d)$ .** We now describe the orthonormal basis in  $L^2(-d, d)$  of [22] and [25, section 6.2.3], which was mentioned in section 1. Consider the set of linearly independent functions  $\{\alpha^s e^{\alpha}\}_{s=0}^{\infty}$ . This set is complete in the space  $L^2(-d, d)$ . Applying the Gram-Schmidt orthonormalization procedure to this set, we obtain the orthonormal basis  $\{\Psi_s(\alpha)\}_{s=0}^{\infty}$  in  $L_2(-d, d)$ . The function  $\Psi_s(\alpha)$  has the form  $\Psi_s(\alpha) = P_s(\alpha) e^{\alpha}$  for all  $s \geq 0$ , where  $P_s(\alpha)$  is a polynomial of the degree  $s$ . Even though the Gram-Schmidt orthonormalization procedure is unstable for the infinite number of elements, it is still stable for a nonlarge number of elements, and this was observed in numerical studies of, e.g., [26], [25, Chapters 7, 10, 12] and references cited therein. Consider the  $N \times N$  matrix  $M_N = (a_{s,k})_{(s,k)=(0,0)}^{(N-1, N-1)}$ , where  $a_{s,k} = [\Psi'_s, \Psi_k]$ , where  $[\cdot, \cdot]$  is the scalar product in  $L^2(-d, d)$ . It was proven in [22], [25, section 6.2.3] that  $a_{s,k} = 1$  if  $s = k$ , and  $a_{s,k} = 0$ , if  $s < k$ . Hence,  $\det M_N = 1$ . Hence, the matrix  $M_N$  is invertible.

*Remark 3.1.* The invertibility of the matrix  $M_N$  is the single most important property of the orthonormal basis  $\{\Psi_s(\alpha)\}_{s=0}^{\infty}$ . Consider, for example, any basis of either classical orthonormal polynomials or orthonormal trigonometric functions in  $L_2(-d, d)$ . Since the first function of such a basis is a constant, then the first row of the analogue  $\widetilde{M}_N$  of the matrix  $M_N$  consists of zeros only. Hence, the matrix  $\widetilde{M}_N$  is not invertible.

**3.3. A coupled system of nonlinear integral differential equations.** Represent the function  $w(\mathbf{x}, \alpha)$  as truncated Fourier series with respect to the above basis  $\{\Psi_s(\alpha)\}_{s=0}^\infty$  and also assume that the derivative  $w_\alpha(\mathbf{x}, \alpha)$  can be represented as the sum of the term-by-term derivatives of that series,

$$(3.7) \quad w(\mathbf{x}, \alpha) = \sum_{s=0}^{N-1} w_s(\mathbf{x}) \Psi_s(\alpha), \quad w_\alpha(\mathbf{x}, \alpha) = \sum_{s=0}^{N-1} w_s(\mathbf{x}) \Psi'_s(\alpha).$$

Therefore, we now need to find the vector function  $W(\mathbf{x}) = (w_0, \dots, w_{N-1})^T(\mathbf{x})$  of coefficients  $w_s(\mathbf{x})$ . Dividing (3.5) by  $\nu_{n+1}(\mathbf{x}, \alpha)$  and then substituting (3.7), we obtain

$$(3.8) \quad \begin{aligned} & \sum_{s=0}^{N-1} \partial_y w_s(\mathbf{x}) \Psi'_s(\alpha) + \frac{\partial_\alpha \nu_{n+1}(\mathbf{x}, \alpha)}{\nu_{n+1}(\mathbf{x}, \alpha)} \sum_{s=0}^{N-1} \partial_y w_{sy}(\mathbf{x}) \Psi_n(\alpha) \\ & + \sum_{s=0}^{N-1} \sum_{i=1}^n \frac{\nu_i(\mathbf{x}, \alpha)}{\nu_{n+1}(\mathbf{x}, \alpha)} \partial_{x_i} w_s(\mathbf{x}) \Psi'_s(\alpha) + \sum_{s=0}^{N-1} \sum_{i=1}^n \frac{\partial_\alpha \nu_i(\mathbf{x}, \alpha)}{\nu_{n+1}(\mathbf{x}, \alpha)} \partial_{x_i} w_s(\mathbf{x}) \Psi_s(\alpha) \\ & - \frac{\mu_s(\mathbf{x})}{\nu_{n+1}(\mathbf{x}, \alpha)} \frac{\partial}{\partial \alpha} \left[ e^{-w(\mathbf{x}, \alpha)} \int_{\Gamma_d} K(\mathbf{x}, \alpha, \beta) e^{w(\mathbf{x}, \beta)} d\beta \right] = 0, \quad \mathbf{x} \in \Omega, \alpha \in (-d, d), \end{aligned}$$

where the function  $w(\mathbf{x}, \alpha)$  in the last line of (3.8) has the form (3.7). The new equation (3.8) does not contain the unknown coefficient  $a(\mathbf{x})$ . Using (3.3), (3.4), and (3.7), we obtain the boundary condition for the vector function  $W(\mathbf{x})$ ,

$$(3.9) \quad W(\mathbf{x})|_{\partial\Omega} = P(\mathbf{x}) = (p_0, \dots, p_{N-1})^T(\mathbf{x}),$$

$$(3.10) \quad p_s(\mathbf{x}) = \int_{-d}^d \ln[g_1(\mathbf{x}, \alpha)] \Psi_s(\alpha) d\alpha, \quad s = 0, \dots, N-1.$$

We need now to solve problem (3.8)–(3.10) with respect to the vector function  $W(\mathbf{x})$ . Multiply sequentially (3.8) by functions  $\Psi_k(\alpha)$ ,  $k = 0, \dots, N-1$ , and integrate with respect to  $\alpha \in (-d, d)$ . We obtain

$$(3.11) \quad (M_N + A_{n+1}(\mathbf{x})) W_y(\mathbf{x}) + \sum_{i=1}^n A_i(\mathbf{x}) W_{x_i}(\mathbf{x}) + F(W(\mathbf{x}), \mathbf{x}) = 0, \quad \mathbf{x} \in \Omega,$$

where  $A_{n+1} \in C_{N^2}(\overline{\Omega})$  and  $A_i \in C_{N^2}(\overline{\Omega})$ ,  $i = 1, \dots, n$ , are  $N \times N$  matrices, and the  $N$ -D vector function

$$(3.12) \quad F(s, x) \in C^2(\mathbb{R}^{N+n+1})$$

is generated by the operator in the last line of (3.8). Here, (3.12) follows from (2.14), (2.15), (2.17), (3.5), and (3.8). Obviously the vector function  $F(W(\mathbf{x}), \mathbf{x})$  is nonlinear with respect to  $W(\mathbf{x})$ . By (3.6) and (3.8)

$$(3.13) \quad \|A_i(\mathbf{x})\|_{C_{N^2}(\overline{\Omega})} \leq C/a,$$

where the number  $C = C(A, d, N, b) > 0$  depends only on listed parameters.

Denote

$$(3.14) \quad D_N(\mathbf{x}) = (M_N + A_{n+1}(\mathbf{x})) = M_N (I + M_N^{-1} A_1(\mathbf{x})).$$

Since the matrix  $M_N$  is invertible, then it follows from (2.1) and (3.13) that there exists such a number  $a_0 = a_0(A, d, M_N) > 1$  depending only on listed parameters that

$$(3.15) \quad \text{the matrix } D_N^{-1}(\mathbf{x}) \text{ exists for all } a \geq a_0 \text{ and for all } \mathbf{x} \in \bar{\Omega}.$$

**3.4. Approximate mathematical model.** We discuss in this subsection the truncation of the Fourier-like series (3.7).

1. We use in this paper an approximate mathematical model, which amounts to the truncation of the Fourier-like series (3.7). We do not know how to prove convergence of our method in the case when the number of terms of this series  $N \rightarrow \infty$ .
2. Thus, in fact, we work with a version of the Galerkin method. One can also call this a “projection method” with  $N$  unknown functions  $\{w_s(\mathbf{x})\}_{s=0}^{N-1}$ . In both cases convergence when  $N \rightarrow \infty$  is not proven.
3. Truncations of Fourier-like series with respect to the same basis  $\{\Psi_s(\alpha)\}_{s=0}^{\infty}$  as the one above were done in [20, 26], [25, Chapters 7, 10, 12] for various versions of the convexification method for a variety of CIPs.
4. We refer to works of some other authors [15, 17, 18, 19], which discuss some other inverse problems and use truncated Fourier series without proofs of convergence when  $N \rightarrow \infty$ .
5. The *fundamental* reason of one’s inability to provide such proofs is the ill-posed nature of the underlying inverse problems.
6. Therefore, the *only way* to verify the validity of such approximate mathematical models is via numerical experiments, as in section 6 as well as in the past works cited in item 4.
7. Conceptually, the issue discussed in this subsection is quite similar to with the well-known issue of the theory of Huygens and Fresnel of the diffraction in optics since this model is yet not derived rigorously from the Maxwell’s equations. On the other hand, since the entire optical industry is based on the theory of Huygens and Fresnel, then obviously a good performance of this theory is well verified in practice. Somewhat similarly, we verify our approximate mathematical model numerically in section 6.
8. To support the discussion of item 7, we now cite some statements on pages 412 and 413 of the classical textbook of Nobel prize laureate Max Born and Emil Wolf [5]: “*Diffraction problems are amongst most difficult ones encountered in optics.... Because of mathematical difficulties, approximate methods must be used in most cases of practical interest. Of these the theory of Huygens and Fresnel is by far most powerful and is adequate for the treatment of the majority of problems encountered in instrumental optics.*” Here, the term “approximate methods” has the same meaning as our term “approximate mathematical model.”
9. We assume below that the derivatives  $W_{x_i}, i = 1, \dots, n$ , in (3.11) are written in finite differences with the grid step size  $h \geq h_0 > 0$ , where the number  $h_0$  is fixed. On the other hand, the  $y$ -derivative is understood in the conventional sense. The assumption

$h \geq h_0$  is a reasonable one since one does not allow the grid step sizes to tend to zero in practical computations. This assumption is the second element, in addition to (3.7), of our approximate mathematical model.

**3.5. Partial finite differences.** Let  $m > 1$  be an integer. Consider  $n$  partitions of the interval  $(-A, A)$  (see (2.2)):

$$(3.16) \quad -A = x_{i,0} < x_{i,1} < \cdots < x_{i,m} = A, x_{i,j+1} - x_{i,j} = h, j = 0, \dots, m-1, i = 1, \dots, n.$$

We assume that

$$(3.17) \quad h \geq h_0 = \text{const.} > 0.$$

Define the semidiscrete subset  $\Omega^h$  of the domain  $\Omega$  as

$$(3.18) \quad \Omega_1^h = \{x_{i,j}\}_{(i,j)=(1,0)}^{(i,j)=(n,m)},$$

$$(3.19) \quad \Omega^h = \Omega_1^h \times (a, b) = \left\{ (x_{i,j}, y) : \{x_{i,j}\}_{(i,j)=(1,0)}^{(i,j)=(n,m)} \in \Omega_1^h, y \in (a, b) \right\}.$$

We denote  $\mathbf{x}^h = \{(x_{i,j}, y) : x_{i,j} \in \Omega_1^h, y \in (a, b)\}$ . By (2.3)–(2.5) and (3.18), (3.19) the boundary  $\partial\Omega^h$  of the domain  $\Omega^h$  is

$$\begin{aligned} \partial\Omega^h &= \partial_1\Omega^h \cup \partial_2\Omega^h \cup \partial_3\Omega^h, \\ \partial_1\Omega^h &= \Omega_1^h \times \{y = a\}, \quad \partial_2\Omega^h = \Omega_1^h \times \{y = b\}, \\ \partial_3\Omega^h &= \{(x_{i,0}, y), (x_{i,m}, y) : y \in (a, b), i = 1, \dots, n\}. \end{aligned}$$

Let the vector function  $Q(\mathbf{x}) \in C_N^1(\bar{\Omega})$ . Denote

$$\begin{aligned} Q_{ij}^h(y) &= Q(x_{i,j}, y), i = 1, \dots, n; j = 0, \dots, m; y \in (a, b), \\ Q^h(\mathbf{x}^h) &= \left\{ Q^h(x_{1,j}, x_{2,j}, \dots, x_{n,j}, y) \right\}, y \in (a, b). \end{aligned}$$

Thus,  $Q^h(\mathbf{x}^h)$  is an  $N - D$  vector function of discrete variables  $x_{i,j} \in \Omega^h$  and continuous variable  $y \in (a, b)$ . Note that the boundary terms at  $\partial_3\Omega^h$  of this vector function, which correspond to  $Q(\mathbf{x})|_{\partial_3\Omega^h}$ , are  $\{Q_{i,0}^h(y)\} \cup \{Q_{i,m}^h(y)\}, i = 1, \dots, n$ . For two vector functions  $Q^{(1)}(\mathbf{x}) = (Q_1^{(1)}(\mathbf{x}), \dots, Q_N^{(1)}(\mathbf{x}))^T$  and  $Q^{(2)}(\mathbf{x}) = (Q_1^{(2)}(\mathbf{x}), \dots, Q_N^{(2)}(\mathbf{x}))^T$  their scalar product  $Q^{(1)}(\mathbf{x}) \cdot Q^{(2)}(\mathbf{x})$  is defined as the scalar product in  $\mathbb{R}^N$  and  $(Q^{(1)}(\mathbf{x}))^2 = Q^{(1)}(\mathbf{x}) \cdot Q^{(1)}(\mathbf{x})$ . Respectively,

$$(3.20) \quad Q^{(1)h}(\mathbf{x}^h) \cdot Q^{(2)h}(\mathbf{x}^h) = \sum_{k=1}^N \sum_{(i,j)=(1,1)}^{(i,j)=(1,m-1)} Q_k^{(1)h}(x_{i,j}, y) Q_k^{(2)h}(x_{i,j}, y),$$

$$(3.21) \quad \left( Q^h(\mathbf{x}^h) \right)^2 = Q^h(\mathbf{x}^h) \cdot Q^h(\mathbf{x}^h), \quad |Q^h(\mathbf{x}^h)| = \sqrt{Q^h(\mathbf{x}^h) \cdot Q^h(\mathbf{x}^h)}.$$

We will use formulas (3.20), (3.21) everywhere below without further mention. We exclude  $j = 0$  and  $j = m$  here since we work below with finite difference derivatives as defined in the next paragraph.

We define finite difference derivatives of  $Q^h(\mathbf{x}^h)$  with respect to  $x_1, \dots, x_n$  only at interior points of the domain  $\Omega^h$  with as

(3.22)

$$\begin{aligned} \partial_{x_k} Q^h(\mathbf{x}^h) &= Q_{x_k}^h(\mathbf{x}^h) = \left\{ Q^h(x_{1,j}, x_{2,j}, \dots, x_{n,j}, y) \right\}_{x_k} \\ &= \left\{ \frac{Q^h(x_{1,j}, \dots, x_{k-1,j}, x_{k,j+1}, x_{k+1,j}, \dots, x_{n,j}, y) - Q^h(x_{1,j}, \dots, x_{k-1,j}, x_{k,j-1}, x_{k+1,j}, \dots, x_{n,j}, y)}{2h} \right\}. \end{aligned}$$

The second line of (3.22) should be adjusted in an obvious fashion for  $k = 1$  and  $k = n$ . Also, in that line  $j = 1, \dots, m - 1$ . We need semidiscrete analogues of spaces  $C_N(\overline{\Omega})$ ,  $H_N^1(\Omega)$ , and  $L_N^2(\Omega)$ . All of them are defined using the same principle; see, e.g., [20] for these definitions. As an example, we introduce the space  $H_N^{1,h}(\Omega^h)$  and its subspace  $H_{N,0}^{1,h}(\Omega^h)$ . Others are similar.

$$\begin{aligned} H_N^{1,h}(\Omega^h) &= \left\{ \begin{array}{c} Q^h(\mathbf{x}^h) : \|Q^h(\mathbf{x}^h)\|_{H_N^{1,h}(\Omega^h)}^2 \\ = \sum_{(i,j,k)=(1,1,1)}^{(i,j,k)=(n,m-1,n)} \int_a^b \left[ \left( Q_{ij}^h(y) \right)^2 + \left( Q_{x_k}^h(\mathbf{x}^h) \right)^2 + \left( \partial_y Q_{ij}^h(y) \right)^2 \right] dy < \infty \end{array} \right\}, \\ H_{N,0}^{1,h}(\Omega^h) &= \left\{ Q^h(\mathbf{x}^h) \in H_N^{1,h}(\Omega^h) : Q^h(\mathbf{x}^h)|_{\partial\Omega^h} = 0 \right\}. \end{aligned}$$

By the embedding theorem  $H_N^{1,h}(\Omega^h) \subset C_N^h(\overline{\Omega^h})$  and

$$(3.23) \quad \|Q^h(\mathbf{x}^h)\|_{C_N^h(\overline{\Omega^h})} \leq C_1 \|Q^h(\mathbf{x}^h)\|_{H_N^{1,h}(\overline{\Omega^h})} \quad \forall Q^h \in H_N^{1,h}(\Omega^h),$$

where the number  $C_1 = C_1(h_0, A, a, b, \Omega) > 0$  depends only on listed parameters, and the number  $h_0$  is defined in (3.17).

**Remark 3.2.** Since we work with finite difference derivatives (3.22) only at interior points of the discrete domain  $\Omega^h$ , then in any differential operator below we use  $W^h(\mathbf{x}^h) = \{W_{ij}^h(y)\}_{(i,j)=(1,1)}^{(i,j)=(n,m-1)}, y \in (a, b)$ , i.e., boundary points  $x_{i,0}$  and  $x_{i,m}$  are involved only in finite difference derivatives  $W_i^h(\mathbf{x}^h)$  at  $x_{i,1}$  and  $x_{i,m-1}$ . Points  $x_{i,0}$  and  $x_{i,m}$  are not included in (3.20) for the same reason.

Using (3.16)–(3.22), we now rewrite problem (3.9)–(3.11) in the form of finite differences with respect to  $x_1, \dots, x_n$  as

$$(3.24) \quad D_N^h(\mathbf{x}^h) W_y^h(\mathbf{x}^h) + \sum_{i=1}^n A_i^h(\mathbf{x}^h) W_{x_i}^h(\mathbf{x}^h) + F^h(W^h(\mathbf{x}^h), \mathbf{x}^h) = 0, \quad \mathbf{x}^h \in \Omega^h,$$

$$(3.25) \quad W^h(\mathbf{x}^h)|_{\partial\Omega^h} = P^h(\mathbf{x}^h).$$

In (3.24)  $N \times N$  matrices  $A_i^h(\mathbf{x}^h) \in C_N(\overline{\Omega^h})$ , the matrix  $D_N^h(\mathbf{x}^h) \in C(\overline{\Omega^h})$  is the semidiscrete analogue of the matrix  $D_N(\mathbf{x})$  defined in (3.14). By (3.13) and (3.14)

$$(3.26) \quad \|D_N^h\|_{C_{N^2}^h(\overline{\Omega^h})} \leq C_2 \quad \forall a \geq a_0 = a_0(A, d, N) > 1.$$

The vector function  $F^h(W^h(\mathbf{x}^h), \mathbf{x}^h)$  is the semidiscrete analogue of the vector function  $F$  in (3.11), and by (3.12)  $F^h(W^h(\mathbf{x}^h), \mathbf{x}^h)$  is twice continuously differentiable with respect to components of  $W^h(\mathbf{x}^h)$ . By (3.15) there exists the inverse matrix  $(D_N^h)^{-1}(\mathbf{x}^h)$  and

$$(3.27) \quad \left\| \left( D_N^h \right)^{-1} \right\|_{C_{N^2}^h(\overline{\Omega^h})} \leq C_2 \quad \forall a \geq a_0 = a_0(A, d, N) > 1.$$

Furthermore, (3.13) and (3.27) imply for  $i = 1, \dots, n$

$$(3.28) \quad \left\| \left( \left( D_N^h \right)^{-1} A_i^h \right) (\mathbf{x}^h) \right\|_{C_{N^2}^h(\overline{\Omega^h})} \leq C_2 \quad \forall a \geq a_0 = a_0(A, d, N) > 1,$$

Here and everywhere below  $C_2 = C_2(A, d, N, a, b, h_0, \|K\|_{C^1(\overline{\Omega} \times [-d, d]^2)}) > 0$  denotes different constants depending only on listed parameters.

The following formulas are semidiscrete analogues of (3.7):

$$(3.29) \quad w^h(\mathbf{x}^h, \alpha) = \sum_{n=0}^{N-1} w_n^h(\mathbf{x}^h) \Psi_n(\alpha), \quad \partial_\alpha w^h(\mathbf{x}^h, \alpha) = \sum_{n=0}^{N-1} w_n^h(\mathbf{x}^h) \Psi'_n(\alpha).$$

We also denote  $W^h(\mathbf{x}^h) = (w_0^h, \dots, w_{N-1}^h)^T(\mathbf{x}^h)$ . Suppose that we have found this vector. Then, to find the semidiscrete analogue  $a^h(\mathbf{x}^h)$  of the unknown coefficient  $a(\mathbf{x})$ , we use (3.29) and (3.29) as

$$(3.30) \quad \begin{aligned} a^h(\mathbf{x}^h) &= -\frac{1}{2d} \int_{-d}^d \nu(\mathbf{x}^h, \alpha) \cdot \nabla_{\mathbf{x}^h} w^h(\mathbf{x}^h, \alpha) d\alpha \\ &+ \frac{1}{2d} \int_{-d}^d \left( e^{-w^h(\mathbf{x}^h, \alpha)} \mu_s(\mathbf{x}^h) \int_{-d}^d K(\mathbf{x}^h, \alpha, \beta) e^{w^h(\mathbf{x}^h, \beta)} d\beta \right) d\alpha, \quad \mathbf{x}^h \in \Omega^h. \end{aligned}$$

**4. Convexification method for problem (3.24), (3.25).** Let  $R > 0$  be an arbitrary number. Define the set  $B(R, P^h)$  as

$$(4.1) \quad B(R, P^h) = \left\{ W^h \in H_N^{1,h}(\Omega^h) : W^h(\mathbf{x}^h) |_{\partial\Omega^h} = P^h(\mathbf{x}^h), \left\| W^h \right\|_{H_N^{1,h}(\Omega^h)} < R \right\},$$

where  $P^h(\mathbf{x}^h)$  is the boundary condition in (3.25). Consider matrices  $G_i^h(\mathbf{x}^h)$  and the vector function  $\Phi^h(W^h(\mathbf{x}^h), \mathbf{x}^h)$ ,

$$(4.2) \quad G_i^h(\mathbf{x}^h) = \left( \left( D_N^h \right)^{-1} A_i^h \right) (\mathbf{x}^h),$$

$$(4.3) \quad \Phi^h \left( W^h(\mathbf{x}^h), \mathbf{x}^h \right) = \left( D_N^h(\mathbf{x}^h) \right)^{-1} F^h \left( W^h(\mathbf{x}^h), \mathbf{x}^h \right).$$

By (3.12), (3.27), (3.28), (4.1)–(4.3), and the multidimensional analogue of Taylor formula [34]

$$(4.4) \quad \left\| G_i^h(\mathbf{x}^h) \right\|_{C_{N^2}^h(\overline{\Omega^h})} \leq C_2 \quad \forall a \geq a_0 > 1, \quad i = 1, \dots, n,$$

$$(4.5) \quad \left\| \Phi^h \left( W^h(\mathbf{x}^h), \mathbf{x}^h \right) \right\|_{C_N^h(\overline{\Omega^h})} \leq C_2 \quad \forall W^h \in \overline{B(R, P^h)},$$

$$(4.6) \quad \begin{aligned} \Phi^h \left( W_2^h(\mathbf{x}^h), \mathbf{x}^h \right) &= \Phi^h \left( W_1^h(\mathbf{x}^h), \mathbf{x}^h \right) + \Phi_1 \left( W_1^h(\mathbf{x}^h), \mathbf{x}^h \right) \left( W_2^h - W_1^h \right) (\mathbf{x}^h) \\ &+ \Phi_2^h \left( W_1^h(\mathbf{x}^h), W_2^h(\mathbf{x}^h), \mathbf{x}^h \right) \quad \forall W_1^h, W_2^h \in \overline{B(R, P^h)} \quad \forall \mathbf{x}^h \in \overline{\Omega^h}, \end{aligned}$$

where the vector function  $\Phi_1(W_1^h(\mathbf{x}^h), \mathbf{x}^h)$  is independent on  $W_2^h(\mathbf{x}^h)$ , the vector function  $\Phi_2^h(W_1^h(\mathbf{x}^h), W_2^h(\mathbf{x}^h), \mathbf{x}^h)$  is nonlinear with respect to  $(W_2^h - W_1^h)(\mathbf{x}^h)$ , both these vector functions are continuous with respect to their variables for  $\mathbf{x}^h \in \Omega^h$ , and the following estimates hold for all  $W_1^h, W_2^h \in \overline{B(R, P^h)}$  and for all  $\mathbf{x}^h \in \Omega^h$  (also see (3.21)):

$$(4.7) \quad \left| \Phi_1 \left( W_1^h(\mathbf{x}^h), \mathbf{x}^h \right) \right| \leq C_2 \quad \forall W_1^h \in \overline{B(R, P^h)} \quad \forall \mathbf{x}^h \in \Omega^h,$$

$$(4.8) \quad \left| \Phi_2^h \left( W_1^h(\mathbf{x}^h), W_2^h(\mathbf{x}^h), \mathbf{x}^h \right) \right| \leq C_2 \left( W_2^h - W_1^h \right)^2 (\mathbf{x}^h) \quad \forall \mathbf{x}^h \in \Omega^h.$$

**Lemma 4.1.** *Let  $A$  be a  $k \times k$  matrix which has the inverse  $A^{-1}$ . Then there exists a number  $\mu = \mu(A) > 0$  such that  $\|Ax\|^2 \geq \mu\|x\|^2$  for all  $x \in \mathbb{R}^k$ , where  $\|\cdot\|$  is the euclidean norm.*

We omit the proof since this lemma is well known.

**Corollary 4.1.** *The following inequality holds:*

$$\begin{aligned} &\left( D_N^h(\mathbf{x}^h) W_y^h(\mathbf{x}^h) + \sum_{i=1}^n A_i^h(\mathbf{x}^h) W_{x_i}^h(\mathbf{x}^h) \right)^2 \\ &\geq C_2 \left( W_y^h(\mathbf{x}^h) + \sum_{i=1}^n G_i^h(\mathbf{x}^h) W_{x_i}^h(\mathbf{x}^h) \right)^2 \quad \forall \mathbf{x}^h \in \Omega^h. \end{aligned}$$

**Proof.** Denote

$$(4.9) \quad Y(\mathbf{x}^h) = W_y^h(\mathbf{x}^h) + \sum_{i=1}^n G_i^h(\mathbf{x}^h) W_{x_i}^h(\mathbf{x}^h) + \Phi^h \left( W^h(\mathbf{x}^h), \mathbf{x}^h \right).$$

We have

$$(4.10) \quad \left( D_N^h(\mathbf{x}^h) W_y^h(\mathbf{x}^h) + \sum_{i=1}^n A_i^h(\mathbf{x}^h) W_{x_i}^h(\mathbf{x}^h) \right)^2 = \left( D_N^h(\mathbf{x}^h) Y(\mathbf{x}^h) \right)^2.$$

The rest of the proof follows immediately from (4.2), (4.3), and Lemma 4.1. ■

Introduce the following weighted cost functional  $J_\lambda(W^h)$ :

$$(4.11) \quad J_\lambda(W^h) = \left\| \left( D_N^h W_y^h + \sum_{i=1}^n A_i^h W_{x_i}^h + F^h \left( W^h(\mathbf{x}^h), \mathbf{x}^h \right) \right) e^{\lambda y} \right\|_{L_N^{2,h}(\Omega^h)}^2.$$

**Minimization problem.** Minimize functional (4.11) on the set  $\overline{B(R, P^h)}$ .

Theorems 4.1–4.5 are our analytical results about the functional  $J_\lambda(W^h)$ .

**Theorem 4.1 (Carleman estimate).** *Assume that the number  $a \geq a_0$ , as in (3.27). Then there exists a sufficiently large number  $\lambda_0 = \lambda_0(A, d, N, a, b, h_0) \geq 1$  depending only on listed parameters such that the following Carleman estimate holds:*

$$(4.12) \quad \begin{aligned} & \left\| \left( W_y^h(\mathbf{x}^h) + \sum_{i=1}^n G_i^h(\mathbf{x}^h) W_{x_i}^h(\mathbf{x}^h) \right) e^{\lambda y} \right\|_{L_N^{2,h}(\Omega^h)}^2 \\ & \geq \left\| W_y^h e^{\lambda y} \right\|_{L_N^{2,h}(\Omega^h)}^2 + \lambda^2 \left\| W^h e^{\lambda y} \right\|_{L_N^{2,h}(\Omega^h)}^2 \quad \forall W^h \in H_{N,0}^{1,h}(\Omega^h) \forall \lambda \geq \lambda_0. \end{aligned}$$

**Theorem 4.2 (the central analytical result).** *The following three assertions hold:*

1. *The functional  $J_\lambda(W^h)$  in (4.11) has the Fréchet derivative  $J'_\lambda(W^h) \in H_{N,0}^{1,h}(\Omega^h)$  at any point  $W^h \in \overline{B(R, P^h)}$  and for any value of the parameter  $\lambda \geq 0$ . The Lipschitz condition holds,*

$$(4.13) \quad \left\| J'_\lambda(W_1^h) - J'_\lambda(W_2^h) \right\|_{H_{N,0}^{1,h}(\Omega^h)} \leq C_3 \left\| W_1^h - W_2^h \right\|_{H_{N,0}^{1,h}(\Omega^h)} \quad \forall W_1^h, W_2^h \in \overline{B(R, P^h)}$$

for all  $\lambda \geq 0$ , where the number  $C_3 > 0$  depends on the same parameters as the ones in  $C_2$  as well as on  $\lambda$ .

Assume that the number  $a \geq a_0$ , as in (3.27). Then,

2. *there exists a sufficiently large number  $\lambda_1$*

$$(4.14) \quad \lambda_1 = \lambda_1(R, A, d, N, a, b, h_0) \geq \lambda_0 \geq 1$$

depending only on listed parameters such that the functional  $J_\lambda(W^h)$  in (4.11) is strictly convex on the set  $\overline{B(R, P^h)}$ , i.e., the following inequality holds:

$$(4.15) \quad J_\lambda(W_2^h) - J_\lambda(W_1^h) - J'_\lambda(W_1^h)(W_2^h - W_1^h) \geq C_2 e^{2\lambda a} \left\| W_2^h - W_1^h \right\|_{H_{N,0}^{1,h}(\Omega^h)}^2$$

$$(4.16) \quad \forall \lambda \geq \lambda_1 \quad \forall W_1^h, W_2^h \in \overline{B(R, P^h)}.$$

3. *For each  $\lambda \geq \lambda_1$  there exists unique minimizer  $W_{\min,\lambda}^h \in \overline{B(R, P^h)}$  of the functional  $J_\lambda(W^h)$  on the set  $\overline{B(R, P^h)}$ . Furthermore, the following inequality holds:*

$$(4.17) \quad J'_\lambda(W_{\min,\lambda}^h)(W^h - W_{\min,\lambda}^h) \geq 0 \quad \forall W^h \in \overline{B(R, P^h)}.$$

Theorem 4.3 follows immediately from (4.15) and (4.16). This is a certain uniqueness result for our CIP, which is obtained as a by-product. A further discussion of the uniqueness issue is outside of the scope of this paper.

**Theorem 4.3.** *Assume that the number  $a \geq a_0$ , as in (3.27). Then there exists at most one pair of functions  $(W^h, a^h) \in H_N^{1,h}(\Omega^h) \times L_N^{2,h}(\Omega^h)$  satisfying conditions (3.24), (3.30).*

We now estimate the accuracy of the minimizer  $W_{\min,\lambda}^h$  depending on the level of the noise  $\delta > 0$  in the data. Following the concept of Tikhonov for ill-posed problems [33], we assume the existence of the exact solution

$$(4.18) \quad W^{h*} \in B(R, P^{h*})$$

of problem (3.24)–(3.25) with the exact, i.e., noiseless data  $P^{h*}$ , i.e., for  $\mathbf{x}^h \in \Omega^h$

$$(4.19) \quad D_N^h(\mathbf{x}^h)W_y^{h*}(\mathbf{x}^h) + \sum_{i=1}^n A_i^h(\mathbf{x}^h)W_{x_i}^{h*}(\mathbf{x}^h) + F^h(W^{h*}(\mathbf{x}^h), \mathbf{x}^h) = 0,$$

$$(4.20) \quad W^{h*}(\mathbf{x}^h)|_{\partial\Omega^h} = P^{h*}(\mathbf{x}^h).$$

Suppose that there exists a vector function  $S^h \in H_N^{1,h}(\Omega^h)$  such that

$$(4.21) \quad S^h(\mathbf{x}^h)|_{\partial\Omega^h} = P^h(\mathbf{x}^h), \quad \|S^h\|_{H_N^{1,h}(\Omega^h)} < R.$$

Let  $S^{h*} \in H_N^{1,h}(\Omega^h)$  be such a vector function that

$$(4.22) \quad S^{h*}(\mathbf{x}^h)|_{\partial\Omega^h} = P^{h*}(\mathbf{x}^h), \quad \|S^{h*}\|_{H_N^{1,h}(\Omega^h)} < R.$$

We assume that

$$(4.23) \quad \|S^h - S^{h*}\|_{H_N^{1,h}(\Omega^h)} < \delta.$$

**Theorem 4.4.** *Assume that the number  $a \geq a_0$ , as in (3.27). Suppose that conditions (4.19)–(4.23) hold. Also, consider the number  $\lambda_2$ ,*

$$(4.24) \quad \lambda_2 = \lambda_1(2R, A, d, N, a, b, h_0),$$

where  $\lambda_1(R, A, d, N, a, b, h_0)$  is the number in (4.14). Let  $W_{\min, \lambda_2}^h$  be the minimizer of functional (4.11) on the set  $\overline{B(R, P^h)}$ , which was found in Theorem 4.2. Let  $\alpha \in (0, R)$  be a number. Suppose that (4.18) is replaced with

$$(4.25) \quad W^{h*} \in B(R - \alpha, P^{h*}) \text{ and } C_2\delta < \alpha.$$

Then the vector function  $W_{\min, \lambda_2}^h$  belongs to the open set  $B(R, P^h)$  and the following accuracy estimate holds:

$$(4.26) \quad \|W_{\min, \lambda_2}^h - W^{h*}\|_{H_N^{1,h}(\Omega^h)} \leq C_2\delta.$$

Consider now the gradient descent method of the minimization of functional (4.11) on the set  $\overline{B(R, P^h)}$ . Let  $W_0^h \in B(R/3, P^h)$  be an arbitrary point of this set. We treat it as the starting point of the latter method. The sequence of this method is

$$(4.27) \quad W_n^h = W_{n-1}^h - \gamma J'_{\lambda_2}(W_{n-1}^h), \quad n = 1, 2, \dots,$$

where  $\gamma > 0$  is a small number and  $\lambda_2$  is the same as in (4.24). Note that since by Theorem 4.2 functions  $J'_{\lambda_2}(W_{n-1}^h) \in H_{N,0}^{1,h}(\Omega^h)$ , then all vector functions  $W_n^h$  have the same boundary conditions  $P^h$ .

**Theorem 4.5.** *Let conditions of Theorem 4.4 hold, except that (4.25) is replaced with*

$$(4.28) \quad W^{h*} \in B\left((R - \alpha)/3, P^{h*}\right) \text{ and } C_2\delta < \alpha/3.$$

*Then there exists a sufficiently small number  $\gamma > 0$  and a number  $\theta = \theta(\gamma) \in (0, 1)$  such that in (4.27) all functions  $W_n^h \in B(R, P^h)$  and the following convergence estimates hold:*

$$(4.29) \quad \|W_n^h - W_{\min, \lambda_2}^h\|_{H_N^{1,h}(\Omega^h)} \leq \theta^n \|W_0^h - W_{\min, \lambda_2}^h\|_{H_N^{1,h}(\Omega^h)},$$

$$(4.30) \quad \|W_n^h - W^{h*}\|_{H_N^{1,h}(\Omega^h)} \leq C_2\delta + \theta^n \|W_0^h - W_{\min, \lambda_2}^h\|_{H_N^{1,h}(\Omega^h)},$$

$$(4.31) \quad \|a_n^h - a^{h*}\|_{L_N^{2,h}(\Omega^h)} \leq C_2\delta + \theta^n \|W_0^h - W_{\min, \lambda_2}^h\|_{H_N^{1,h}(\Omega^h)},$$

where  $a_n^h(\mathbf{x}^h)$  and  $a^{h*}(\mathbf{x}^h)$  are functions which are obtained from  $W_n^h$  and  $W^{h*}$ , respectively, via (3.29) and (3.30).

**Remark 4.1.** 1. Estimates (4.29)–(4.31) guarantee the global convergence of the gradient descent method (4.27) since  $R > 0$  is an arbitrary number and the starting point  $W_0^h$  is an arbitrary point of the set  $B(R/3, P^h)$ ; see section 1 for our definition of the global convergence. Note that, for a nonconvex functional, any gradient-like method converges only locally, i.e., it needs a good first guess about the correct solution.

2. Although the above results are valid only for sufficiently large values of the parameter  $\lambda$ , we have established computationally in section 6 that  $\lambda = 5$  works quite well; also, see Remark 6.1 in section 6. It was computationally established in a number of previous works on the convexification that values  $\lambda \in [1, 3]$  work well numerically; see, e.g., [20, 24, 26], [25, Chapters 7–10], and references cited therein. In other words, computationally appropriate intervals for  $\lambda$  were found in these works.

3. Conceptually, the situation, which is somewhat analogous to with the one of item 2, occurs in many asymptotic theories. Typically an asymptotic theory claims that if a certain parameter  $X_1$  is sufficiently large/small, then a certain formula  $X_2$  is valid with a good accuracy. However, for any specific mathematical problem with its specific range of parameters only computational experiments can establish which values of  $X_1$  guarantee a good accuracy of  $X_2$ .

**5. Proofs.** We use in this section (3.20)–(3.22) and Remark 3.2 without further mention.

**5.1. Proof of Theorem 4.1.** In this proof,  $W^h \in H_{N,0}^{1,h}(\Omega^h)$  is an arbitrary function. It follows from (3.17) and (3.22) that

$$(5.1) \quad \|W_{x_i}^h e^{\lambda y}\|_{L_N^{2,h}(\Omega^h)}^2 \leq C_2 \|W^h e^{\lambda y}\|_{L_N^{2,h}(\Omega^h)}^2 \quad \forall W^h \in H_{N,0}^{1,h}(\Omega^h).$$

By (4.4) and (5.1)

$$(5.2) \quad \left\| \left( \sum_{i=1}^n G_i^h(\mathbf{x}^h) W_{x_i}^h(\mathbf{x}^h) \right) e^{\lambda y} \right\|_{L_N^{2,h}(\Omega^h)}^2 \leq C_2 \|W^h e^{\lambda y}\|_{L_N^{2,h}(\Omega^h)}^2.$$

Using the Cauchy–Schwarz inequality and (5.2), we obtain

$$(5.3) \quad \begin{aligned} & \left\| \left( W_y^h(\mathbf{x}^h) + \sum_{i=1}^n G_i^h(\mathbf{x}^h) W_{x_i}^h(\mathbf{x}^h) \right) e^{\lambda y} \right\|_{L_N^{2,h}(\Omega^h)}^2 \\ & \geq C_{2,1} \left\| W_y^h e^{\lambda y} \right\|_{L_N^{2,h}(\Omega^h)}^2 - C_{2,2} \left\| W^h e^{\lambda y} \right\|_{L_N^{2,h}(\Omega^h)}^2. \end{aligned}$$

It makes sense to use two numbers  $C_{2,1}, C_{2,2} > 0$  here; both depend on the same parameters as the ones in  $C_2$ . Consider now the first term in the second line of (5.3). Introduce a new vector function  $V^h(\mathbf{x}^h) = W^h(\mathbf{x}^h)e^{\lambda y}$ . Then

$$\begin{aligned} W^h(\mathbf{x}^h) &= V^h(\mathbf{x}^h) e^{-\lambda y}, \quad W_y^h(\mathbf{x}^h) = \left( V_y^h(\mathbf{x}^h) - \lambda V^h(\mathbf{x}^h) \right) e^{-\lambda y}, \\ \left( W_y^h(\mathbf{x}^h) \right)^2 e^{2\lambda y} &= \left( V_y^h(\mathbf{x}^h) - \lambda V^h(\mathbf{x}^h) \right)^2 \geq -2\lambda V_y^h(\mathbf{x}^h) V^h(\mathbf{x}^h) + \lambda^2 \left( V^h(\mathbf{x}^h) \right)^2 \\ &= \partial_y \left( -\lambda V^h(\mathbf{x}^h) \right)^2 + \lambda^2 \left( V^h(\mathbf{x}^h) \right)^2. \end{aligned}$$

Integrating the latter inequality with respect to  $y \in (a, b)$ , using the fact that  $W^h(\mathbf{x}^h) = V^h(\mathbf{x}^h) = 0$  for  $y = a, b$ , and coming back from  $V^h(\mathbf{x}^h)$  to  $W^h(\mathbf{x}^h)$ , we obtain

$$(5.4) \quad \left\| W_y^h e^{\lambda y} \right\|_{L_N^{2,h}(\Omega^h)}^2 \geq \lambda^2 \left\| W^h e^{\lambda y} \right\|_{L_N^{2,h}(\Omega^h)}^2.$$

Adding the term  $\|W_y^h e^{\lambda y}\|_{L_N^{2,h}(\Omega^h)}^2$  to both sides of (5.4) and then dividing by 2, we obtain for all  $\lambda > 0$

$$(5.5) \quad \left\| W_y^h e^{\lambda y} \right\|_{L_N^{2,h}(\Omega^h)}^2 \geq \frac{1}{2} \left\| W_y^h e^{\lambda y} \right\|_{L_N^{2,h}(\Omega^h)}^2 + \frac{\lambda^2}{2} \left\| W^h e^{\lambda y} \right\|_{L_N^{2,h}(\Omega^h)}^2.$$

Hence, taking  $\lambda_0^2 \geq 2C_{2,2}/C_{2,1}$ ,  $\lambda \geq \lambda_0$  and using (5.3) and (5.5), we obtain (4.12).

**5.2. Proof of Theorem 4.2.** Let  $W_1^h(\mathbf{x}^h), W_2^h(\mathbf{x}^h) \in \overline{B(R, P^h)}$  be two arbitrary points. Denote  $v^h(\mathbf{x}^h) = W_2^h(\mathbf{x}^h) - W_1^h(\mathbf{x}^h)$ . By (4.1)

$$(5.6) \quad v^h \in H_{N,0}^{1,h}(\Omega^h).$$

By (4.11)

$$(5.7) \quad \begin{aligned} J_\lambda \left( W_2^h \right) &= J_\lambda \left( W_1^h + v^h \right) \\ &= \left\| \left( D_N^h \left( W_{1y}^h + v_y^h \right) + \sum_{i=1}^n A_i^h \left( W_{1x_i}^h + v_{x_i}^h \right) + F^h \left( \left( W^h + v^h \right), \mathbf{x}^h \right) \right)^2 e^{\lambda y} \right\|_{L_N^{2,h}(\Omega^h)}^2. \end{aligned}$$

Consider the expression under the sign of the norm in (5.7) without, however, the term  $e^{\lambda y}$ . By (4.2), (4.3), (4.9), and (4.10)

$$(5.8) \quad \begin{aligned} & \left( D_N^h \left( W_{1y}^h + v_y^h \right) + \sum_{i=1}^n A_i^h(\mathbf{x}^h) \left( W_{1x_i}^h + v_{x_i}^h \right) + F^h \left( W^h + v^h, \mathbf{x}^h \right) \right)^2 \\ &= \left[ D_N^h \left( \left( W_{1y}^h + v_y^h \right) + \sum_{i=1}^n G_i^h \left( W_{1x_i}^h + v_{x_i}^h \right) + \Phi^h \left( W_1^h + v^h, \mathbf{x}^h \right) \right) \right]^2. \end{aligned}$$

Consider the term  $\Phi^h(W_1^h + v^h, \mathbf{x}^h)$ . By (4.6)–(4.8) we have for all  $\mathbf{x}^h \in \Omega^h$

$$(5.9) \quad \Phi^h(W_1^h + v^h, \mathbf{x}^h) = \Phi^h(W_1^h, \mathbf{x}^h) + \Phi_1(W_1^h, \mathbf{x}^h) v^h(\mathbf{x}^h) + \Phi_2(W_1^h, W_1^h + v^h, \mathbf{x}^h),$$

$$(5.10) \quad \left| \Phi_1(W_1^h, \mathbf{x}^h) \right| \leq C_3, \quad \left| \Phi_2(W_1^h, W_1^h + v^h, \mathbf{x}^h) \right| \leq C_3 (v^h(\mathbf{x}^h))^2.$$

It follows from (5.9) and (5.10) that the second line of (5.8) is

$$(5.11) \quad \begin{aligned} & \left[ D_N^h \left( (W_{1y}^h + v_y^h) + \sum_{i=1}^n G_i^h (W_{1x_i}^h + v_{x_i}^h) + \Phi^h(W_1^h, \mathbf{x}^h) \right) \right]^2 \\ &= \left[ D_N^h \left( W_{1y}^h + \sum_{i=1}^n G_i^h W_{1x_i}^h + \Phi^h(W_1^h, \mathbf{x}^h) \right) \right]^2 \\ &+ 2D_N^h \left( W_{1y}^h + \sum_{i=1}^n G_i^h W_{1x_i}^h + \Phi^h(W_1^h, \mathbf{x}^h) \right) \\ &\cdot D_N^h \left( v_y^h + \sum_{i=1}^n G_i^h v_{x_i}^h + \Phi_1(W_1^h, \mathbf{x}^h) v^h(\mathbf{x}^h) \right) \\ &+ 2D_N^h \left( W_{1y}^h + \sum_{i=1}^n G_i^h W_{1x_i}^h + \Phi^h(W_1^h, \mathbf{x}^h) \right) \cdot \left( D_N^h \Phi_2^h(W_1^h, W_1^h + v^h, \mathbf{x}^h) \right) \\ &+ \left[ D_N^h \left( v_y^h + \sum_{i=1}^n G_i^h v_{x_i}^h + \Phi_1(W_1^h, \mathbf{x}^h) v^h(\mathbf{x}^h) + \Phi_2(W_1^h, W_1^h + v^h, \mathbf{x}^h) \right) \right]^2. \end{aligned}$$

In (5.11) “.” means the scalar product in the appropriate euclidean space. The linear with respect to  $v^h$  term in (5.11) is the scalar product of the third and fourth lines of this equality. We denote the latter as  $Lin(v^h(\mathbf{x}^h), \mathbf{x}^h)$ . The sum of the fifth and sixth lines of (5.11) contains only nonlinear terms with respect to  $v^h$ . We denote this sum as  $Nonlin(v^h(\mathbf{x}^h), \mathbf{x}^h)$ . It follows from Corollary 4.1, (3.26), (4.2)–(4.8), (5.10), the fifth and sixth lines of (5.11), and the Cauchy–Schwarz inequality that

$$(5.12) \quad \left| Nonlin(v^h(\mathbf{x}^h), \mathbf{x}^h) \right| \geq C_{2,3} \left( v_y^h + \sum_{i=1}^n G_i^h v_{x_i}^h \right)^2 - C_{2,4} (v^h(\mathbf{x}^h))^2 \quad \forall \mathbf{x}^h \in \overline{\Omega^h}.$$

Just as in the proof of Theorem 4.1, it again makes sense to use two positive constants  $C_{2,3}, C_{2,4} > 0$  here, both depending on the same parameters as the ones involved in  $C_2$ . Taking into account (5.7), (5.8), and (5.11), we obtain

(5.13)

$$\begin{aligned} J_\lambda(W_2^h) &= J_\lambda(W_1^h + v^h) = J_\lambda(W_1^h) \\ &+ \sum_{(i,j)=(1,1)}^{(i,j)=(n,m-1)} \int_a^b Lin(v^h(\mathbf{x}^h), \mathbf{x}^h) e^{2\lambda y} dy + \sum_{(i,j)=(1,1)}^{(i,j)=(n,m-1)} \int_a^b Nonlin(v^h(\mathbf{x}^h), \mathbf{x}^h) e^{2\lambda y} dy. \end{aligned}$$

It follows from (4.4)–(4.6), (5.6), and the third and fourth lines of (5.11), which form  $\text{Lin}(v^h(\mathbf{x}^h), \mathbf{x}^h)$ , that the first term in the second line of (5.13) is a bounded linear functional with respect to  $v^h$  mapping  $H_{N,0}^{1,h}(\Omega^h)$  in  $\mathbb{R}$ . We denote this functional as  $\tilde{J}_\lambda(W_1^h)(v^h)$ . By the Riesz theorem there exists unique function  $J'_\lambda(W_1^h) \in H_{N,0}^{1,h}(\Omega^h)$  such that

$$(5.14) \quad \tilde{J}_\lambda(W_1^h)(v^h) = (J'_\lambda(W_1^h), v^h) \quad \forall v^h \in H_{N,0}^{1,h}(\Omega^h),$$

where  $(\cdot, \cdot)$  is the scalar product in  $H_{N,0}^{1,h}(\Omega^h)$ . It follows from (3.27), (3.28), (4.4)–(4.7), and the fifth and sixth lines of (5.11) combined with (5.10) that for  $\|v^h\|_{H_N^{1,h}(\Omega^h)} < 1$

$$\left| \sum_{(i,j)=(1,1)}^{(i,j)=(n,m-1)} \int_a^b \text{Nonlin} \left( v^h(\mathbf{x}^h), \mathbf{x}^h \right) e^{2\lambda y} dy \right| \leq C_2 e^{2\lambda b} \|v^h\|_{H_N^{1,h}(\Omega^h)}^2.$$

Hence, (5.13) implies that

$$\frac{J_\lambda(W_1^h + v^h) - J_\lambda(W_1^h) - (J'_\lambda(W_1^h), v^h)}{\|v^h\|_{H_N^{1,h}(\Omega^h)}} = O \left( \|v^h\|_{H_N^{1,h}(\Omega^h)} \right) \text{ as } \|v^h\|_{H_N^{1,h}(\Omega^h)} \rightarrow 0.$$

Thus,  $J'_\lambda(W_1^h) : H_{N,0}^{1,h}(\Omega^h) \rightarrow \mathbb{R}$  is the Fréchet derivative of the functional  $J_\lambda(W^h)$  at the point  $W_1^h$ . We omit the proof of estimate (4.13) since this proof is completely similar to the proof of Theorem 3.1 of [1].

We now prove (4.15), (4.16). Using (5.12)–(5.14), we obtain

$$(5.15) \quad \begin{aligned} & J_\lambda(W_1^h + v^h) - J_\lambda(W_1^h) - (J'_\lambda(W_1^h), v^h) \\ & \geq C_{2,3} \left\| \left( v_y^h + \sum_{i=1}^n G_i^h v_{x_i}^h \right) e^{\lambda y} \right\|_{L_N^{2,h}(\Omega^h)}^2 - C_{2,4} \|v^h e^{\lambda y}\|_{L_N^{2,h}(\Omega^h)}^2. \end{aligned}$$

Let the number  $\lambda_0$  be the one chosen in Theorem 4.1. Recalling (5.6) and using Theorem 4.1, we estimate the second line of (5.15) for all  $\lambda \geq \lambda_0$  as

$$(5.16) \quad \begin{aligned} & C_{2,3} \left\| \left( v_y^h + \sum_{i=1}^n G_i^h v_{x_i}^h \right) e^{\lambda y} \right\|_{L_N^{2,h}(\Omega^h)}^2 - C_{2,4} \|v^h e^{\lambda y}\|_{L_N^{2,h}(\Omega^h)}^2 \\ & \geq C_2 \left( \|v_y^h e^{\lambda y}\|_{L_N^{2,h}(\Omega^h)}^2 + \lambda^2 \|v^h e^{\lambda y}\|_{L_N^{2,h}(\Omega^h)}^2 \right) - C_{2,4} \|v^h e^{\lambda y}\|_{L_N^{2,h}(\Omega^h)}^2. \end{aligned}$$

Choosing  $\lambda_1 \geq \lambda_0$  so large that  $\lambda_1^2 C_2 / 2 > 2C_{2,4}$  and using (5.16), we obtain

$$(5.17) \quad \begin{aligned} & C_{2,3} \left\| \left( v_y^h + \sum_{i=1}^n G_i^h v_{x_i}^h \right) e^{\lambda y} \right\|_{L_N^{2,h}(\Omega^h)}^2 - C_{2,4} \|v^h e^{\lambda y}\|_{L_N^{2,h}(\Omega^h)}^2 \\ & \geq C_2 \left( \|v_y^h e^{\lambda y}\|_{L_N^{2,h}(\Omega^h)}^2 + \lambda^2 \|v^h e^{\lambda y}\|_{L_N^{2,h}(\Omega^h)}^2 \right). \end{aligned}$$

Combining (5.15) with (5.17), we obtain (4.15), (4.16).

Finally, given (4.15) and (4.16), existence and uniqueness of the minimizer  $W_{\min,\lambda}^h$  of the functional  $J_\lambda(W^h)$  on the set  $\overline{B(R, P^h)}$  as well as estimate (4.17) follow immediately from a combination of Lemma 2.1 with Theorem 2.1 of [1].

### 5.3. Proof of Theorem 4.4.

Denote

$$(5.18) \quad B_0(2R) = \left\{ V^h \in H_{N,0}^{1,h}(\Omega^h) : \|V^h\|_{H_N^{1,h}(\Omega^h)} < 2R \right\}.$$

Consider the vector functions  $V^{h*}$  and  $V^h$ ,

$$(5.19) \quad V^{h*} = W^{h*} - S^{h*}, \quad V^h = W^h - S^h \quad \forall W^h \in B(R, P^h).$$

By (4.18), (4.21), (4.22), (5.18), and (5.19)

$$(5.20) \quad V^h, V^{h*} \in B_0(2R).$$

Consider now the functional  $I_\lambda(V^h)$ ,

$$(5.21) \quad I_\lambda(V^h) : B_0(2R) \rightarrow \mathbb{R}, \quad I_\lambda(V^h) = J_\lambda(V^h + S^h).$$

An obvious analogue of Theorem 4.2 holds for  $I_\lambda(V^h)$ . However, it follows from (5.20) that we need to replace  $R$  with  $2R$  in (4.14) in this case, i.e., we need to use now the number  $\lambda_2$  in (4.24). Let  $V_{\min,\lambda_2}^h$  be the minimizer of  $I_{\lambda_2}(V^h)$  on the set  $B_0(2R)$ .

Consider  $I_\lambda(V^{h*}) = J_\lambda(V^{h*} + S^h)$ . By (4.15), (4.16), and (5.21)

$$I_{\lambda_2}(V^{h*}) - I_{\lambda_2}(V_{\min,\lambda_2}^h) - I'_{\lambda_2}(V_{\min,\lambda_2}^h)(V^{h*} - V_{\min,\lambda_2}^h) \geq C_2 \|V^{h*} - V_{\min,\lambda_2}^h\|_{H_N^{1,h}(\Omega^h)}^2.$$

By (4.17)  $-I'_{\lambda_2}(V_{\min,\lambda_2}^h)(V^{h*} - V_{\min,\lambda_2}^h) \leq 0$ . Since  $-I_{\lambda_2}(V_{\min,\lambda_2}^h) \leq 0$  as well, then the latter estimate implies

$$(5.22) \quad \|V^{h*} - V_{\min,\lambda_2}^h\|_{H_N^{1,h}(\Omega^h)}^2 \leq C_2 I_{\lambda_2}(V^{h*}).$$

Next, by (5.19) and (5.21)

$$(5.23) \quad I_{\lambda_2}(V^{h*}) = J_{\lambda_2}(V^{h*} + S^h) = J_{\lambda_2}(W^{h*} + (S^h - S^{h*})).$$

By (4.19) the right-hand side of (4.11) equals zero if  $W^h$  is replaced with  $W^{h*}$ . Hence, using (4.2)–(4.8), (4.23), and (5.19), we obtain  $J_{\lambda_2}(W^{h*} + (S^h - S^{h*})) \leq C_3 \delta^2$ . Hence, (5.22) and (5.23) lead to

$$(5.24) \quad \|V^{h*} - V_{\min,\lambda_2}^h\|_{H_N^{1,h}(\Omega^h)} \leq C_2 \delta.$$

Using again (4.23), (5.19), the triangle inequality, and (5.24), we obtain

$$(5.25) \quad \|W^{h*} - \widetilde{W}_{\min,\lambda_2}^h\|_{H_N^{1,h}(\Omega^h)} \leq C_2 \delta.$$

Here  $\widetilde{W}_{\min, \lambda_2}^h = V_{\min, \lambda_2}^h - S^h$ . By (4.25), (5.25), and the triangle inequality  $\|\widetilde{W}_{\min, \lambda_2}^h\|_{H_N^{1,h}(\Omega^h)} < R$ . Hence, (4.1), (4.21), (5.18), and (5.20) imply that

$$(5.26) \quad \widetilde{W}_{\min, \lambda_2}^h \in B(R, P^h).$$

Now, let  $W_{\min, \lambda_2}^h$  be the minimizer of the functional  $J_{\lambda_2}(W^h)$  on the set  $\overline{B(R, P^h)}$ , which is claimed by Theorem 4.2. Let  $Q_{\min, \lambda_2}^h = W_{\min, \lambda_2}^h - S^h$ . Then  $Q_{\min, \lambda_2}^h \in B_0(2R)$ . Hence,

$$J_{\lambda_2}(\widetilde{W}_{\min, \lambda_2}^h) = J_{\lambda_2}(V_{\min, \lambda_2}^h + G) \leq J_{\lambda_2}(Q_{\min, \lambda_2}^h + G) = \min_{\overline{B(R, P^h)}} J_{\lambda_2}(W^h).$$

Hence, by (5.26)  $\widetilde{W}_{\min, \lambda_2}^h$  is also a minimizer of the functional  $J_{\lambda_2}(W^h)$  on the set  $\overline{B(R, P^h)}$ . However, since such a minimizer is unique by Theorem 4.2, then  $\widetilde{W}_{\min, \lambda_2}^h = W_{\min, \lambda_2}^h \in B(R, P^h)$ . Hence, estimate (5.25) holds when  $\widetilde{W}_{\min, \lambda_2}^h$  is replaced with  $W_{\min, \lambda_2}^h$ . The latter immediately implies (4.26).

**5.4. Proof of Theorem 4.5.** Consider again the minimizer  $W_{\min, \lambda_2}^h$  of the functional  $J_{\lambda_2}(W^h)$  on the set  $\overline{B(R, P^h)}$ . Then (4.28) and Theorem 4.4 imply that  $W_{\min, \lambda_2}^h \in B(R/3, P^h)$ . Estimate (4.29) follows immediately from Theorem 6 of [24]. Next, by the triangle inequality, (4.26), and (4.29)

$$\begin{aligned} \|W_n^h - W^{h*}\|_{H_N^{1,h}(\Omega^h)} &\leq \|W_{\min, \lambda_2}^h - W^{h*}\|_{H_N^{1,h}(\Omega^h)} + \|W_n^h - W_{\min, \lambda_2}^h\|_{H_N^{1,h}(\Omega^h)} \\ &\leq C_2 \delta + \theta^n \|W_0^h - W_{\min, \lambda_2}^h\|_{H_N^{1,h}(\Omega^h)}, \end{aligned}$$

which proves (4.30). Estimate (4.31) follows immediately from (3.29), (3.30), and (4.30).

**6. Numerical studies.** In order not to introduce new and complicated notation, we slightly abuse below some notation of the previous sections. Nevertheless, the substance is always clear from the context presented below.

**6.1. Numerical implementation.** We have conducted our numerical studies in the two-dimensional case. Below  $\mathbf{x} = (x, y)$  and, according to (2.2) and (2.6),

$$(6.1) \quad \begin{aligned} \Omega &= \{\mathbf{x} : x \in (-A, A), y \in (a, b)\}, \quad A = 1/2, \quad a = 1, \quad b = 2, \\ \Gamma_d &= \{\mathbf{x}_\alpha = (\alpha, 0) : \alpha \in [-d, d]\}, \quad d = 1/2. \end{aligned}$$

As to the kernel  $K(\mathbf{x}, \alpha, \beta)$  of the integral operator in (2.12), we work below with the two-dimensional Henyey-Greenstein function [16]:

$$(6.2) \quad K(\mathbf{x}, \alpha, \beta) = H(\alpha, \beta) = \frac{1}{2d} \left[ \frac{1 - g^2}{1 + g^2 - 2g \cos(\alpha - \beta)} \right], \quad g = \frac{1}{2}.$$

Here,  $g = 1/2$  means an anisotropic scattering, which is half ballistic with  $g = 0$  and half isotropic scattering with  $g = 1$  [10, 11, 12]. We take the same function  $f(\mathbf{x})$  as the one in (2.7), (2.8) with  $\varepsilon = 0.05$ .

We assume that

$$(6.3) \quad \mu_s(\mathbf{x}) = 5, \quad \mathbf{x} \in \Omega, \quad \mu_s(\mathbf{x}) = 0, \quad \mathbf{x} \in \mathbb{R}^2 \setminus \Omega.$$

We use formula (2.15) for the coefficient function  $a(\mathbf{x})$ , and we take in this formula

$$(6.4) \quad \mu_a(\mathbf{x}) = \begin{cases} c = \text{const.} > 0 & \text{inside the tested inclusion,} \\ 0 & \text{outside the tested inclusion.} \end{cases}$$

We perform the numerical tests with a variety of values of the parameter  $c = 5, 10, 15, 20, 30$ ; see below. Therefore, by (2.15), (6.3), and (6.4)

$$(6.5) \quad \text{inclusion/background contrast} = 1 + c/5.$$

From the physics standpoint  $\mu_s(\mathbf{x}) = 5$  in the domain  $\Omega$ , as in (6.3), means that an average particle scatters every  $1/5$  of the unit. Hence, by (6.1) and (6.3) the maximal average number of scattering events for a particle emitted from a point  $\mathbf{x}_\alpha \in \Gamma_d$  and entering  $\Omega$  is around 5 before this particle leaves  $\Omega$  [10, 11, 12]. This might happen in optics before the true diffusion occurs, e.g., in the case of the so-called snake photons [9].

In computational results below the computed function  $\mu_{a,comp}(\mathbf{x})$  does not have a constant value inside of computed shapes of letters, as it should by (6.4). Hence, for computed inclusion/background contrasts we replace (6.5) with

$$(6.6) \quad \text{computed inclusion/background contrast} = 1 + 0.2 \max_{\bar{\Omega}} \mu_a(\mathbf{x}).$$

By (2.10) and (6.1) we have in our case  $G_a^+ = \{\mathbf{x} = (x, y) : |x| < 1/2, y \in (1, 2)\}$ . To solve the forward problem formulated in section 2, we have solved integral equation (2.33) with condition (2.34) for  $(\mathbf{x}, \alpha) \in G_a^+ \times (-d, d)$  and with the function  $u_0(\mathbf{x}, \alpha)$  taken from (2.30). To do this, we have used the discrete form of (2.30), (2.33) and the trapezoidal rule. The discretization steps with respect to  $x, y, \alpha$  were  $h_x = h_y = h_\alpha = 1/40$ . The discretized integral equation (2.33) was solved as a linear system using the MATLAB function \|. Thus, the solution of this forward problem has provided us with computationally simulated data for the inverse problem.

To minimize the convexification functional  $J_\lambda(W^h)$  in (4.11), we have written in the finite differences form not only the  $x$ -derivative as in section 4 but the  $y$ -derivative as well. Also, integrals with respect to  $\alpha$  were written in the discrete form using the trapezoidal rule. Then we have minimized the resulting functional  $J_{\lambda,dis}(W^h)$ ,

$$(6.7) \quad J_{\lambda,dis}(W^h) = \left\| \left( D_N^h W_y^h + A^h W_x^h + F^h \left( W^h(\mathbf{x}^h), \mathbf{x}^h \right) \right) e^{\lambda y} \right\|_{L_N^{2,h}(\Omega^h)}^2,$$

in its fully discrete form with respect to the values of the vector function  $W^h$  at the grid points. Vector functions and matrices in (6.7) are full analogues of those in (4.11) with the only difference that they are fully discrete in the above sense, rather than “partially” discrete as in sections 4 and 5. The same is true for the norm  $\|\cdot\|_{L_N^{2,h}(\Omega^h)}$ .

The mesh sizes were different from ones for the forward problem. They were  $h_x = h_y = h_\alpha = h = 1/20$ . Hence, by (6.1) we had a total of  $20 \times 20 \times N$  unknown parameters in our

minimization procedure. To solve the minimization problem, we have used the MATLAB built-in function **fminunc** with the quasi-Newton algorithm. The iterations of the function **fminunc** were stopped when the following inequality occurred at the iteration number  $k$ :

$$\left| J_{\lambda, \text{dis}}(W_k^h) \right| < 10^{-2}.$$

By (3.8) our technique requires computations of first derivatives with respect to  $\alpha$ . Note, however, that (3.7)–(3.10) imply that it is not necessary to calculate the  $\alpha$ -derivative of the boundary data, which is an advantage, since boundary data are noisy. The derivatives  $\partial_\alpha$  of functions  $\Psi_s(\alpha)$  and the function  $K(\mathbf{x}, \alpha, \beta)$  were calculated via finite differences. We have introduced the random noise in the boundary data  $g_1(\mathbf{x}, \alpha)$  in (3.4) on the boundary  $\partial\Omega$ ,

$$(6.8) \quad g_1(\mathbf{x}, \alpha) = g_1(\mathbf{x}, \alpha) (1 + \sigma \zeta_{\mathbf{x}}).$$

Here  $\zeta_{\mathbf{x}}$  is the uniformly distributed random variable in the interval  $[0, 1]$  depending on the point  $\mathbf{x} \in \partial\Omega$  with  $\sigma = 0.03$  and  $\sigma = 0.05$ , which correspond respectively to 3% and 5% noise level.

To solve the minimization problem, we need to provide the starting  $W_0^h(\mathbf{x}^h)$  for iterations. Due to the global convergence property of our method, the vector function  $W_0^h(\mathbf{x}^h) = (w_{0,0}^h(\mathbf{x}^h), w_{1,0}^h(\mathbf{x}^h), \dots, w_{N-1,0}^h(\mathbf{x}^h))^\top$  should not have any information about the exact solution  $W^{h*}(\mathbf{x}^h)$ . On the other hand, due to (4.1), we should have  $W_0^h(\mathbf{x}^h)|_{\partial\Omega^h} = P^h(\mathbf{x}^h)$ . Therefore, in all numerical tests below we choose the starting point as the discrete version of the following vector function:

$$(6.9) \quad \begin{aligned} w_{s,0}(x, y) &= \frac{1}{2} \left( \frac{(A-x)}{2A} w_s(-A, y) + \frac{(x+A)}{2A} w_s(A, y) \right) \\ &+ \frac{1}{2} \left( \frac{(b-y)}{b-a} w_s(x, a) + \frac{(y-a)}{b-a} w_s(x, b) \right), \quad s = 0, \dots, N-1. \end{aligned}$$

Expression (6.9) represents the average of linear interpolations inside of the square  $\Omega$  with respect to the  $\mathbf{x}$ -direction and the  $y$ -direction of the boundary condition for  $w_s(x, y)$ .

**6.2. Numerical results.** Recall that we reconstruct the coefficient  $a(\mathbf{x}) = \mu_s(\mathbf{x}) + \mu_a(\mathbf{x})$ , where true functions  $\mu_s(\mathbf{x})$  and  $\mu_a(\mathbf{x})$  are given in (6.3) and (6.4), respectively. Our results for Tests 1–4 are for noiseless data and the results for Test 5 are for noisy data as in (6.8).

To demonstrate a good performance of our technique, we intentionally test it for rather complicated shapes of inclusions, which are nonconvex and have voids. More precisely, our inclusions are letters  $A$ ,  $\Omega$  and two letters jointly SZ. SZ stands for Shenzhen, the city where the workplace of the third and fourth authors is located. Thus, in our tests the coefficients  $\mu_a(\mathbf{x})$  in (6.4) have shapes of those letters located inside the  $1 \times 1$  square  $\Omega$  defined in (6.1).

**Test 1.** We test the letter  $A$  with  $c = 5$  in (6.4). This is our reference case. More precisely, we use this test to figure out optimal values of parameters  $N$  and  $\lambda$ . As soon as optimal parameters are selected, we use them then for all other tests.

First, we select an appropriate value of  $N$ . To do this, we solve the forward problem (2.12), (2.19) for the case when the functions  $\mu_s(\mathbf{x})$  and  $\mu_a(\mathbf{x})$  are given in (6.3) and (6.4),

**Table 1**

The  $L_2(\Omega)$ -norms of functions  $w_s(\mathbf{x})$ ,  $s = 0, 1, \dots, 11$ , for the reference Test 1 with  $c = 5$  in (6.4).

$s$	0	1	2	3	4	5
$\ w_s(\mathbf{x})\ _{L_2}$	5.7122	1.6383	0.1630	0.0118	0.0091	0.0077
$s$	6	7	8	9	10	11
$\ w_s(\mathbf{x})\ _{L_2}$	0.0067	0.0061	0.0055	0.0057	0.0058	0.0054

respectively, and  $c = 5$  in (6.4). Hence, by (6.5) the inclusion/background contrast is 2:1 in this case. Next, we calculate norms  $\|w_s(\mathbf{x})\|_{L_2(\Omega)}$  and compare them. Recall that functions  $w_s(\mathbf{x})$  were defined in (3.7). We have observed that the  $L_2(\Omega)$ -norm of the function  $w_s(\mathbf{x})$  decreases very rapidly when the number  $s$  is growing. More precisely, we have obtained that

$$(6.10) \quad \frac{\sum_{s=3}^{11} \|w_s(\mathbf{x})\|_{L_2(\Omega)}}{\sum_{s=0}^{11} \|w_s(\mathbf{x})\|_{L_2(\Omega)}} = 0.0084,$$

which means less than 1%. In addition to (6.10), we display in Table 1 the values of norms  $\|w_s(\mathbf{x})\|_{L_2(\Omega)}$  for  $s = 0, \dots, 11$ . One can observe that starting from  $s = 3$ , these norms are much less than those for  $s = 0, 1, 2$ . We conclude, therefore, that we should take in our tests  $N = 3$ .

Next, given the optimal value of  $N = 3$ , we select the optimal value of the parameter  $\lambda$  of the Carleman weight function  $e^{2\lambda y}$  in (6.7). To do this, we test the same letter A with  $c = 5$  inside of it for values of the parameter  $\lambda = 0, 1, 2, 3, 4, 5, 6, 8, 20$ . Our numerical results are presented in Figure 1. We observe that the images have a low quality for  $\lambda = 0, 1$ . Then the quality is improved, and it is stabilized at  $\lambda = 5$ ; see Remark 6.1 for  $\lambda = 20$ . Thus, we treat  $\lambda = 5$  as the optimal value of this parameter. We use this value in all subsequent tests. The value  $\lambda = 5$  tells us that even though our Theorems 4.1–4.5 require sufficiently large values of the parameter  $\lambda$ , the computational practice shows that a reasonable value of  $\lambda$  can be chosen; see items 2 and 3 of Remark 4.1.

**Remark 6.1.** On the other hand, the quality of the reconstructions deteriorates when  $\lambda$  becomes too large. Indeed, testing  $\lambda = 10, 12, 14, 16, 18$  (images are not shown), we have computationally established that the quality of the reconstructions “monotonically” deteriorates starting at  $\lambda = 10$ , and the image quality becomes really low at  $\lambda = 20$ ; see the last image in Figure 1 for  $\lambda = 20$ . This deterioration can be explained by the fact that the Carleman weight function  $f_\lambda(y) = e^{2\lambda y}, y \in [a, b]$ , in (6.7) grows very rapidly with respect to  $y$  for too large values of  $\lambda$ . Hence, roughly speaking, if  $\lambda \gg 1$ , then the values of the integrand in (6.7) have a noticeable impact in that integral only for values of  $y$  near  $\{y = b\}$ . Thus, we have found a computationally appropriate interval of  $\lambda \in [2, 8]$ , for which our numerical technique works well. We again refer to items 2 and 3 of Remark 4.1. In the future, we plan to investigate this question in more detail.

Now we want to demonstrate numerically again that  $N = 3$  is indeed a good choice of  $N$  for our optimal value of  $\lambda = 5$ . Taking  $\lambda = 5$ , we test the same letter A as above with

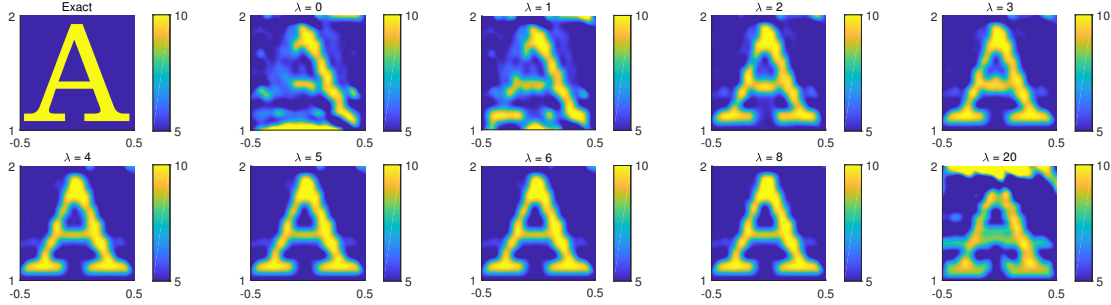


**Figure 1.** The reconstructed coefficient  $a(\mathbf{x})$ , where the function  $\mu_a(\mathbf{x})$  is given in (6.4) with  $c = 5$  inside the letter A. The goal here is to test different values of the parameter  $\lambda = 0, 1, 2, 3, 4, 5, 6, 8, 20$  for  $N = 3$  as in (6.10). The value of  $\lambda$  can be seen on the top side of each square. The images have a low quality for  $\lambda = 0, 1$ . Then the quality is improved and is stabilized at  $\lambda = 5$ . Thus, we select  $\lambda = 5$  as an optimal value of this parameter for all follow up tests. On the other hand, the last image is for the case  $\lambda = 20$ . This image demonstrates that the quality of the reconstructions deteriorates for too large value of  $\lambda$ ; see Remark 6.1 for some details.

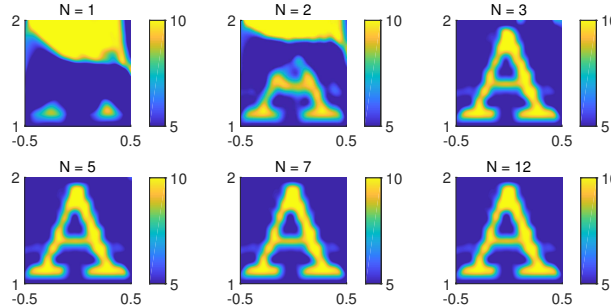


**Figure 2.** The reconstructed coefficient  $a(\mathbf{x})$ , where the function  $\mu_a(\mathbf{x})$  is given in (6.4) with  $c = 5$  inside the letter A. We took the optimal value of the parameter  $\lambda = 5$  (see Figure 1) and have tested different values of the parameter  $N = 1, 2, 3, 5, 7, 12$ . A low quality can be observed for  $N = 1, 2$ . The reconstructions are basically the same for  $N = 3, 5, 7, 12$ . However, the computational cost increases very rapidly with the increase of  $N$ , which is explained by (6.10) and Table 1. We conclude, therefore, that to balance between the reconstruction accuracy and the computational cost, we should use  $N = 3$ . Thus, we use below  $\lambda = 5$  and  $N = 3$ .

$c = 5$  in it, but for  $N = 1, 2, 3, 5, 7, 12$ . The results are displayed in Figure 2. One can observe that reconstructions have a low quality for  $N = 1, 2$ . Next, the reconstructions are basically the same for  $N = 3, 5, 7, 12$ . However, the computational cost increases very rapidly with the increase of  $N$ . Thus, using also Table 1, we conclude that to balance between the reconstruction accuracy and the computational cost, we should use  $N = 3$ . Thus, in all subsequent computations we use

$$(6.11) \quad N = 3, \lambda = 5.$$

**Test 2.** We test the reconstruction of the coefficient  $a(\mathbf{x})$  with the shape of the letter A where the function  $\mu_a(\mathbf{x})$  is given in (6.4) with different values of the parameter  $c = 15, 20, 30$  inside the letter A. Thus, by (6.6) the inclusion/background contrasts now are respectively 4 : 1, 5 : 1, and 6 : 1. Our computational results for this test are displayed in Figure 3. One

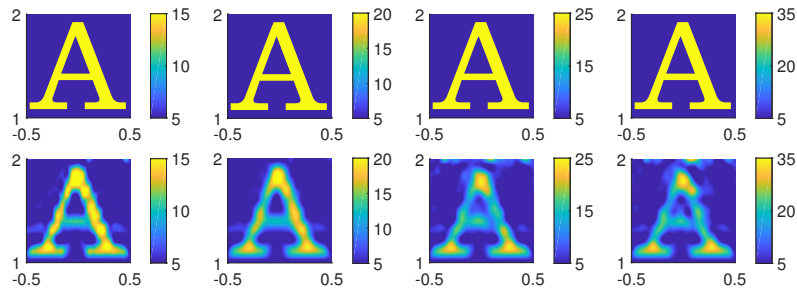


**Figure 3.** Test 2. Exact (top) and reconstructed (bottom) coefficient  $a(\mathbf{x})$  for  $c = 10, 15, 20, 30$  inside the letter A as in (6.4) for  $N = 3, \lambda = 5$ ; see (6.11). Thus, by (6.6) the inclusion/background contrasts now are respectively  $4 : 1$ ,  $5 : 1$ , and  $6 : 1$ . The image quality remains basically the same for all these values of the parameter  $c$ , although some deterioration of this quality can be observed for  $c = 20$  and  $c = 30$ . The computed inclusion/background contrasts (6.6) are accurate.

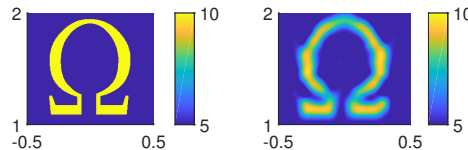


**Figure 4.** Test 3. Exact (left) and reconstructed (right) coefficient  $a(\mathbf{x})$  for the case when the function  $\mu_a(\mathbf{x})$  is given in (6.4) with  $c = 5$  inside the letter  $\Omega$ . The reconstruction is accurate.

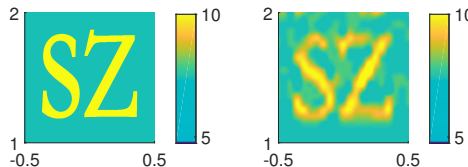


**Figure 5.** Test 4. Exact (left) and reconstructed (right) coefficient  $a(\mathbf{x})$  for the case when the function  $\mu_a(\mathbf{x})$  is given in (6.4) with  $c = 5$  with the shape of two letters SZ. In (6.4)  $c = 5$  inside each of these two letters and  $\mu_a(\mathbf{x}) = 0$  outside each of these two letters. Here  $N = 3, \lambda = 5$  as in (6.11). The image quality is lower than the one for the case of the single letter  $\Omega$  in Figure 4. Nevertheless, the quality is still good and the computed inclusion/background contrasts (6.6) are accurate in both letters.

can observe that the quality of these images is good for all four cases, although it slightly deteriorates for  $c = 20$  and  $c = 30$ . The computed inclusion/background contrast is accurate; see (6.6).

**Test 3.** We test the reconstruction of the coefficient  $a(\mathbf{x})$  with the shape of the letter  $\Omega$  where the function  $\mu_a(\mathbf{x})$  is given in (6.4) with  $c = 5$  inside the letter  $\Omega$ . Results are presented in Figure 4. We again observe an accurate reconstruction.

**Test 4.** We test the reconstruction of the coefficient  $a(\mathbf{x})$  with the shape of two letters SZ where the function  $\mu_a(\mathbf{x})$  is given in (6.4) with  $c = 5$  inside each of these two letters and  $\mu_a(\mathbf{x}) = 0$  outside each of these two letters. In this test,  $N = 3, \lambda = 5$  as in (6.11). Results are presented in Figure 5. The image quality is lower than the one for the case of the single letter  $\Omega$  in Figure 4. Nevertheless, the quality is still good and the computed inclusion/background contrasts (6.6) are accurate in both letters.

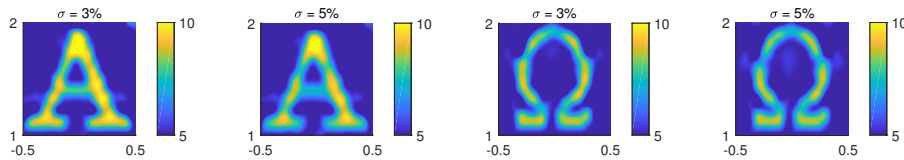


**Figure 6.** Reconstructed coefficient  $a(\mathbf{x})$  with the shape of letters  $A$  and  $\Omega$  with  $c = 5$  from noise polluted observation data as in (6.8) with  $\sigma = 0.03$  and  $\sigma = 0.05$ , i.e., with 3 and 5 noise level. Here  $N = 3$  and  $\lambda = 5$  as in (6.11). One can observe accurate reconstructions in all four cases. In particular, the inclusion/background contrasts (6.6) are reconstructed accurately.

**Test 5.** In this test we use noisy data as in (6.8) with  $\sigma = 0.03$  and  $\sigma = 0.05$ , i.e., with 3% and 5% noise level. We test the reconstruction of the coefficient  $a(\mathbf{x})$  with the shape of either the letter  $A$  or the letter  $\Omega$ , where the function  $\mu_a(\mathbf{x})$  is given in (6.4) with  $c = 5$  inside each of these two letters. Again,  $N = 3$ ,  $\lambda = 5$  as in (6.11). The results are shown in Figure 6. One can observe accurate reconstructions in all four cases. In particular, the inclusion/background contrasts (6.6) are reconstructed accurately.

## REFERENCES

- [1] A. B. BAKUSHINSKII, M. V. KLIBANOV, AND N. A. KOSHEV, *Carleman weight functions for a globally convergent numerical method for ill-posed Cauchy problems for some quasilinear PDEs*, Nonlinear Anal. Real World Appl., 34 (2017), pp. 201–224.
- [2] G. BAL AND A. JOLLIVET, *Generalized stability estimates in inverse transport theory*, Inverse Probl. Imaging, 12 (2018), pp. 59–90.
- [3] G. BAL AND A. TAMASAN, *Inverse source problems in transport equations*, SIAM J. Math. Anal., 39 (2007), pp. 57–76.
- [4] M. BELLASSOUED AND M. YAMAMOTO, *Carleman Estimates and Applications to Inverse Problems for Hyperbolic Systems*, Springer, New York, 2017.
- [5] M. BORN AND E. WOLF, *Principles of Optics*, 7th ed., Cambridge University Press, Cambridge, UK, 1999.
- [6] M. BOULAKIA, M. DE BUHAN, AND E. SCHWINDT, *Numerical reconstruction based on Carleman estimates of a source term in a reaction-diffusion equation*, ESAIM Control Optim. Calc. Var., 27 (2021), pp. 1–34.
- [7] A. L. BUKHGEIM AND M. V. KLIBANOV, *Uniqueness in the large of a class of multidimensional inverse problems*, Sov. Math. Dokl., 17 (1981), pp. 244–247.
- [8] G. CHAVENT, *Nonlinear Least Squares for Inverse Problems: Theoretical Foundations and Step-by-Step Guide for Applications*, Springer Science & Business Media, Berlin, 2010.
- [9] B. B. DAS, F. LIU, AND R. R. ALFANO, *Time-resolved fluorescence and photon migration studies in biomedical and model random media*, Rep. Prog. Phys., 60 (1997), pp. 227–292.
- [10] H. FUJIWARA, K. SADIQ, AND A. TAMASAN, *A Fourier approach to the inverse source problem in an absorbing and anisotropic scattering medium*, Inverse Problems, 36 (2020), 015005.
- [11] H. FUJIWARA, K. SADIQ, AND A. TAMASAN, *Numerical reconstruction of radiative sources in an absorbing and nondiffusing scattering medium in two dimensions*, SIAM J. Imaging Sci., 13 (2020), pp. 535–555.
- [12] H. FUJIWARA, K. SADIQ, AND A. TAMASAN, *A source reconstruction method in two dimensional radiative transport using boundary data measured on an arc*, Inverse Problems, 37 (2021), 115005.
- [13] F. GÖLGELEYEN AND M. YAMAMOTO, *Stability for some inverse problems for transport equations*, SIAM J. Math. Anal., 48 (2016), pp. 2319–2344.
- [14] A. V. GONCHARSKY AND S. Y. ROMANOV, *A method of solving the coefficient inverse problems of wave tomography*, Comput. Math. Appl., 77 (2019), pp. 967–980.

[15] J. GUILLEMENT AND R. G. NOVIKOV, *Inversion of weighted Radon transforms via finite Fourier series weight approximation*, Inverse Probl. Sci. Eng., 22 (2013), pp. 787–802.

[16] J. HEINO, S. ARRIDGE, J. SIKORA, AND E. SOMERSALO, *Anisotropic effects in highly scattering media*, Phys. Rev. E, 68 (2003), 03198.

[17] S. I. KABANIKHIN, N. S. NOVIKOV, I. V. OSELEDETS, AND M. A. SHISHLENIN, *Fast Toeplitz linear system inversion for solving two-dimensional acoustic inverse problem*, J. Inverse Ill-Posed Probl., 23 (2015), pp. 687–700.

[18] S. I. KABANIKHIN, K. K. SABELFELD, N. S. NOVIKOV, AND M. A. SHISHLENIN, *Numerical solution of an inverse problem of coefficient recovering for a wave equation by a stochastic projection methods*, Monte Carlo Methods Appl., 21 (2015), pp. 189–203.

[19] S. I. KABANIKHIN, K. K. SABELFELD, N. S. NOVIKOV, AND M. A. SHISHLENIN, *Numerical solution of the multidimensional Gelfand-Levitin equation*, J. Inverse Ill-Posed Probl., 23 (2015), pp. 439–450.

[20] V. A. KHOA, G. W. BIDNEY, M. V. KLIBANOV, L. H. NGUYEN, A. SULLIVAN, L. NGUYEN, AND V. N. ASTRATOV, *Convexification and experimental data for a 3D inverse scattering problem with the moving point source*, Inverse Problems., 36 (2020), 085007.

[21] M. V. KLIBANOV, *Global convexity in a three-dimensional inverse acoustic problem*, SIAM J. Math. Anal., 28 (1997), pp. 1371–1388.

[22] M. V. KLIBANOV, *Convexification of restricted Dirichlet to Neumann map*, J. Inverse Ill-Posed Probl., 25 (2017), pp. 669–685.

[23] M. V. KLIBANOV AND O. V. IOUSSOPOVA, *Uniform strict convexity of a cost functional for three-dimensional inverse scattering problem*, SIAM J. Math. Anal., 26 (1995), pp. 147–179.

[24] M. V. KLIBANOV, V. A. KHOA, A. V. SMIRNOV, L. H. NGUYEN, G. W. BIDNEY, L. NGUYEN, A. SULLIVAN, AND V. N. ASTRATOV, *Convexification inversion method for nonlinear SAR imaging with experimentally collected data*, J. Appl. Ind. Math., 15 (2021), pp. 413–436.

[25] M. V. KLIBANOV AND J. LI, *Inverse Problems and Carleman Estimates: Global Uniqueness, Global Convergence and Experimental Data*, De Gruyter, Berlin, 2021.

[26] M. V. KLIBANOV, J. LI, AND W. ZHANG, *Electrical impedance tomography with restricted Dirichlet-to-Neumann map data*, Inverse Problems., 35 (2019), 35005.

[27] M. V. KLIBANOV AND S. PAMYATNYKH, *Global uniqueness for a coefficient inverse problem for the non-stationary transport equation via Carleman estimate*, J. Math. Anal. Appl., 343 (2008), pp. 352–365.

[28] R. Y. LAI AND Q. LI, *Parameter reconstruction for general transport equation*, SIAM J. Math. Anal., 52 (2020), pp. 2734–2758.

[29] F. NATTERER, *The Mathematics of Computerized Tomography*, SIAM Publications, Philadelphia, 2001.

[30] R. G. NOVIKOV, *An inversion formula for the attenuated X-ray transformation*, Ark. Mat., 40 (2002), pp. 145–167.

[31] A. V. SMIRNOV, M. V. KLIBANOV, AND L. H. NGUYEN, *On an inverse source problem for the full radiative transfer equation with incomplete data*, SIAM J. Sci. Comput., 41 (2019), pp. B929–B952.

[32] P. STEFANOV AND G. UHLMANN, *An inverse source problem in optical molecular imaging*, Anal. PDE, 1 (2008), pp. 115–126.

[33] A. N. TIKHONOV, A. V. GONCHARSKY, V. V. STEPANOV, AND A. G. YAGOLA, *Numerical Methods for the Solution of Ill-Posed Problems*, Kluwer, London, 1995.

[34] M. M. VAJNBERG, *Variational Method and Method of Monotone Operators in the Theory of Nonlinear Equations*, Israel Program for Scientific Translations, Jerusalem, 1973.